2018

6-Substituted Hexamethylene Amiloride (HMA) Derivatives as Potent and Selective Inhibitors of the Human Urokinase Plasminogen Activator for Use in Cancer

Benjamin J. Buckley
University of Wollongong, bbuckley@uow.edu.au

Ashraf Abdel A. Aboelela
University of Wollongong, ashrafam@uow.edu.au

Elahe Minaei
University of Wollongong, eminaei@uow.edu.au

Longguang Jiang
Fuzhou University

Zhihong Xu
University of New South Wales, Ingram Institute for Applied Medical Research

See next page for additional authors

6-Substituted Hexamethylene Amiloride (HMA) Derivatives as Potent and Selective Inhibitors of the Human Urokinase Plasminogen Activator for Use in Cancer

Abstract

Metastasis is the cause of death in the majority (~90%) of malignant cancers. The oral potassium-sparing diuretic amiloride and its 5-substituted derivative 5-N,N-(hexamethylene)amiloride (HMA) reportedly show robust antitumor/metastasis effects in multiple in vitro and animal models. These effects are likely due, at least in part, to inhibition of the urokinase plasminogen activator (uPA), a key protease determinant of cell invasiveness and metastasis. This study reports the discovery of 6-substituted HMA analogs that show nanomolar potency against uPA, high selectivity over related trypsin-like serine proteases, and minimal inhibitory effects against epithelial sodium channels (ENaC), the diuretic and antikaliuretic target of amiloride. Reductions in lung metastases were demonstrated for two analogs in a late-stage experimental mouse metastasis model, and one analog completely inhibited formation of liver metastases in an orthotopic xenograft mouse model of pancreatic cancer. The results support further evaluation of 6-substituted HMA derivatives as uPA-targeting anticancer drugs.

Disciplines
Medicine and Health Sciences

Authors
Benjamin J. Buckley, Ashraf Abdel A. Aboelela, Elahe Minaei, Longguang Jiang, Zhihong Xu, Umar Ali, Karen J. Fildes, Chen Cheung, Simon M. Cook, Darren Johnson, Daniel Bachovchin, Gregory Cook, Minoti Apte, Mingdong Huang, Marie Ranson, and Michael J. Kelso

6-Substituted hexamethylene amiloride (HMA) derivatives as potent and selective inhibitors of the human urokinase plasminogen activator for use in cancer

Benjamin J. Buckley[|‡], Ashraf Aboelela[|‡], Elahe Minaei[|‡], Longguang X. Jiang[‖], Zhihong Xu[⊥], Umar Ali[|‡], Karen Fildes[‡§], Chen-Yi Cheung[∇], Simon M. Cook[‡], Darren C. Johnson[♦], Daniel A. Bachovchin[♦¥], Gregory M. Cook[∇], Minoti Apte[⊥], Mingdong Huang[‖], Marie Ranson*[|‡] and Michael J. Kelso*[|‡]

[|]Molecular Horizons and School of Chemistry & Molecular Bioscience, University of Wollongong, NSW 2522, Australia.

[‡]Illawarra Health & Medical Research Institute, Wollongong, NSW 2522, Australia.

[§]Graduate School of Medicine, University of Wollongong, NSW 2522, Australia.

[‖]National Joint Biomedical Engineering Research Centre on Photodynamic Technologies, Fuzhou University, Fujian 350116, China.

[⊥]Pancreatic Research Group, South Western Sydney Clinical School, University of New South Wales, and Ingham Institute for Applied Medical Research, NSW 2170, Australia.

[∇]Department of Microbiology and Immunology, University of Otago, Otago 9016, New Zealand.

[♦]Tri-Institutional PhD Program in Chemical Biology, Memorial Sloan Kettering Cancer Center, New York, New York 10065, USA.

[¥]Chemical Biology Program, Memorial Sloan Kettering Cancer Center, New York, New York 10065, USA.

ABSTRACT

Metastasis is the cause of death in the majority (~90%) of malignant cancers. The oral potassium-sparing diuretic amiloride and its 5-substituted derivative 5-*N,N*-(hexamethylene)amiloride (HMA) reportedly show robust anti-tumor/metastasis effects in multiple *in vitro* and animal models. These effects are likely due, at least in part, to inhibition of the urokinase plasminogen activator (uPA), a key protease determinant of cell invasiveness and metastasis. This study reports the discovery of 6-substituted HMA analogs that show nanomolar potency against uPA, high selectivity over related trypsin-like serine proteases and minimal inhibitory effects against epithelial sodium channels (ENaC), the diuretic and anti-kaliuretic target of amiloride. Reductions in lung metastases were demonstrated for two analogs in a late-stage experimental mouse metastasis model and one analog completely inhibited formation of liver metastases in an orthotopic xenograft mouse model of pancreatic cancer. The results support further evaluation of 6-substituted HMA derivatives as uPA-targeting anticancer drugs.

INTRODUCTION

The urokinase plasminogen activator (uPA) is a trypsin-like serine protease (TLSP) that has been implicated in the invasive spread and metastatic dissemination of transformed cells in several aggressive cancers, including triple-negative breast, pancreatic, gastric, colorectal and

prostate cancers.[1-5] Clinically, uPA expression provides the highest level of evidence (Level 1)[6] for predicting poor patient prognosis in breast cancer and it is one of the strongest predictors of progression-free survival and overall survival.[7-9]

uPA binds to cell surfaces via a specific interaction with its cognate receptor urokinase plasminogen activator receptor (uPAR), which is expressed on cancer cells and the supporting stroma, often at the invasive front of tumors.[10-12] uPAR-bound uPA activates co-localised plasminogen to yield the broad spectrum TLSP plasmin,[13] a key mediator of directed pericellular proteolysis that activates multiple downstream proteases (e.g. matrix metalloproteinases and cathepsins), ultimately leading to degradation of the extracellular matrix and basement membrane components that confine primary tumors.[3, 14-15] The uPA-initiated proteolytic cascade is thus a key determinant of local invasion and metastatic spread via the lymphatic and circulatory systems.[16-17]

uPA attracted much interest in the 1990's and early 2000's as an anticancer target in academic and industry labs (reviewed in Ngo *et al.*[18] and Tyndall *et al.*[19]). For example, efforts from Abbott Laboratories led to highly potent naphthamidine-based inhibitors; e.g. **1**.[23-26] X-ray co-crystal structures of these and other inhibitors uncovered a novel subsite, termed S1β, adjacent to the S1 binding pocket in uPA. Targeting of this site afforded potency gains in a variety of aryl amidine-based inhibitors.[23] The poor drug properties of arylamidines ultimately proved to be a major stumbling block, however, and compounds were not advanced to the clinic.[27] Astex Therapeutics were able to repurpose the oral anti-arrhythmic drug mexiletine into a potent, orally active non amidine-containing uPA inhibitor **2**[28] but no clinical studies have been reported to date.

3a and its oral hydroxyamidine prodrug **3b** (Heidelberg Pharma AG; formerly WILEX AG) are, to the best of our knowledge, the only uPA inhibitors to have undergone clinical evaluation in cancer.[29] Phase II studies of oral **3b** in combination with gemcitabine showed a 17% increase in 1-year survival in patients with locally advanced, non-resectable pancreatic cancers compared to patients treated with gemcitabine alone.[30] In a separate Phase II study, patients with HER2-negative metastatic breast cancers who had received adjuvant chemotherapy following primary diagnosis and were subsequently treated with **3b** in combination with capecitabine showed an increase in median progression-free survival (8.3 months) compared to patients receiving capecitabine alone (4.3 months).[31]

Amiloride **4** is an oral potassium-sparing diuretic that has been used for over four decades in the treatment of hypokalemia, hypertension and cirrhosis.[32-33] The diuretic and antikaliuretic properties of amiloride arise through inhibition of renal epithelial sodium channels (ENaCs).[34-35] Several groups have reported that the compound also shows anticancer side-activities in multiple *in vitro* and rodent models (reviewed in Matthews *et al.*).[16] In one study, high doses of amiloride (200 mg/kg in drinking water *ad libitum*) caused complete remission in a prostate xenograft mouse model.[36] It has been suggested that the anticancer effects of amiloride observed at the high doses used in this and other animal studies likely arise, at least in part, from inhibition of uPA proteolytic activity (IC_{50} = 7 μM).[37] Amiloride is unsuitable for use clinically as an anticancer drug, however, due to its low maximum daily dose ceiling (20 mg/day), where overdose risks hyperkalemia and associated cardiac events.[38] Nevertheless, the demonstrable *in vivo* anticancer side-activities of amiloride, combined with excellent drug-like properties (inferred from decades of oral clinical use) and low micromolar potency against uPA, suggest it as an attractive starting scaffold for repurposing using the Selective Optimization of Side-

Activity (SOSA) approach[39] into a high potency uPA inhibitor for treating uPA-driven cancers.[16] Moreover, the reduced basicity of the acyl guanidine group relative to aryl amidines potentially offers a solution to the poor drug properties of earlier inhibitors.[27] We propose that effective dosing of an analog suitably optimized for high uPA potency that lacks the diuretic and anti-kaliuretic effects of amiloride may safely and effectively recapitulate in humans the anticancer activities observed with high doses of amiloride in animals.
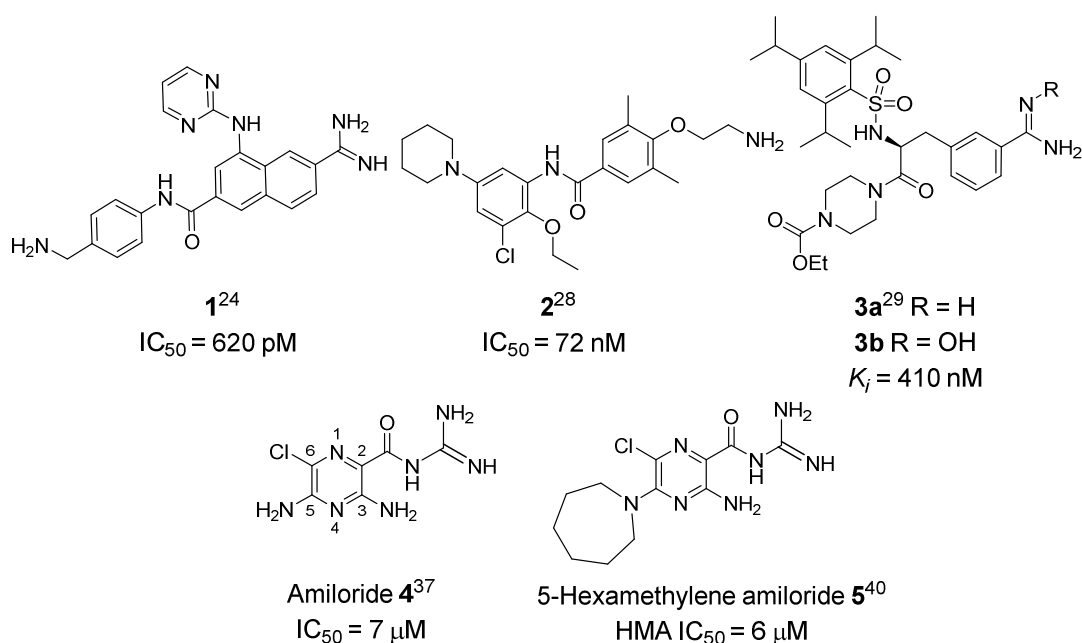
Figure 1. Structures of reported uPA inhibitors.

Our preliminary structure-activity exploration of amiloride analogs as uPA inhibitors focused on the effects of varying substituents at the 5-NH_2 group.[40] Relatively flat SAR trends were observed, with multiple analogs carrying diverse 5-substituents returning IC_{50} values in the range 1-50 μM. Large increases in potency relative to amiloride were not realized, with the most active compound (5-*N,N'*-dimethylethylenediamine amiloride) showing only a ~2-fold increase (IC_{50} =

3 µM). A key finding, however, was that 5-*N,N*-(hexamethylene)amiloride **5** (HMA, Figure 1) retained potency against uPA (IC$_{50}$ = 6 µM).

HMA has a long history of use as a pharmacological tool[41] and, like amiloride, reportedly shows *in vitro* and *in vivo* anti-cancer activities.[42-47] For example, HMA has been shown to delay primary tumor growth and increase thermosensitivity of SCK mammary carcinoma cells in a mouse allograft model,[42, 48] and it was recently shown to suppress sorafenib-resistant engraftment of *FLT3*-ITD+ acute myeloid leukemia primary cells in mice, with total suppression observed in combination with sorafenib.[45] Importantly, alkyl substitution of the 5-NH$_2$ group of amiloride (as in HMA) appears to reduce inhibitory effects against ENaCs.[48-49] Based on this, HMA **5** was selected as the starting point for SOSA optimization.

There have been many structure-activity studies exploring the effects of substitution at various positions around the pyrazine core of amiloride[48] but there is a surprising lack of reports on analogs carrying variations at the 6-position of amiloride, HMA or any other 5-substituted amilorides.[50] This study reports the synthesis, uPA structure-activity relationships and *in vivo* anti-cancer properties of HMA analogs carrying (hetero)aryl substituents at the 6-position.

RESULTS AND DISCUSSION

Chemistry. The reported X-ray co-crystal structure of amiloride bound to uPA[51] indicated that the 6-Cl group projects towards the S1β subsite, suggesting that other groups attached here might better occupy the site and increase potency. A diverse series of 6-(hetero)aryl substituted HMA analogs was produced from the common 5-*N,N*-(hexamethylene)amiloride methyl ester

intermediate **7** (Scheme 1). Ester **7** was obtained via nucleophilic aromatic substitution of the commercially available 3-amino-5,6-dichloropyrazine-2-methyl ester **6** with hexamethyleneimine. The reported method for preparing **7**,[40] which involves heating **6** with hexamethyleneamine in DMF at 100 °C for 1 hour, requires multiple column chromatography steps to obtain pure **7** (65% yield). We found that when the reaction was instead performed at reflux in 2-propanol in the presence of *N*,*N*-diisopropylethylamine (DIPEA), an excellent yield of **7** (86%) was obtained after only 2 hours. The improved procedure could be performed on multi-gram scale in an open flask with the pure **7** crystallizing from the reaction mixture and isolated by simple filtration.

Direct attachment of (hetero)aryl substituents to the 6-position of **7** was achieved using standard Suzuki-Miyaura cross-coupling conditions with commercial aryl boronic acids (or pinacol boronates), $Pd(PPh_3)_4$ and K_2CO_3 in toluene/MeOH (4:1) at reflux. A total of twenty three 6-(hetero)aryl methyl esters **9a**-**32a** were produced in yields ranging from 34-93%. The methyl esters were converted to their respective acylguanidines **9-32** in 2-92% by treatment with guanidine. Low guanidinylation yields were initially obtained using the reported method[40] leading us to search for an improved procedure. Treating the methyl esters in DMF with a 2 M stock solution of guanidine in MeOH was found to give much higher yields, with most reactions proceeding to completion at room temperature and and no major side products forming. The revised procedure was simple to carry out, allowed multiple guanidinylation reactions to be performed in parallel and the 2 M guanidine solution could be stored under N_2 in a refrigerator for up to 2 weeks.[52]

Scheme 1. Synthesis of 6-(hetero)aryl HMA analogs 9-32[a]
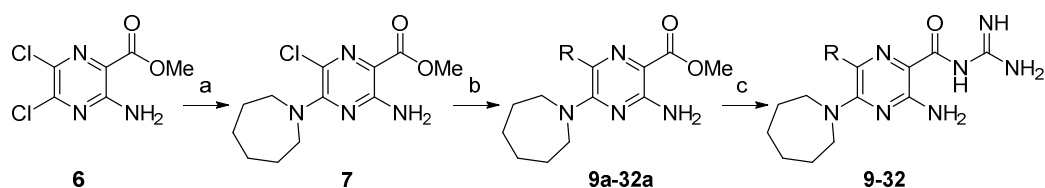
*a*Reagents and conditions: (a) (CH₂)₆NH, DIPEA, ᶦPrOH, reflux, 2 h, 86%; (b) R-B(OH)₂ or R-B(pin), Pd(PPh₃)₄, K₂CO₃, toluene/MeOH (4:1), reflux, 0.5-18 h; (c) guanidine (2 M in MeOH), DMF, rt, 18 h.

6-(2-(Alkylamino)pyrimidin-5-yl) HMA analogs **33-35** (Scheme 2) were obtained from 6-(2-chloropyrimidin-5-yl) methyl ester intermediate **8**. Compound **8** was synthesized in 64% yield by Suzuki-Miyaura coupling of **7** with (2-chloropyrimidin-5-yl)boronic acid. Nucleophilic aromatic substitution of the 2-chloro group with the requisite amines yielded esters **33a-35a** in 83-87% yields, which were converted to acyl guanidines **33-35** in 85-89% yields using the new guanidinylation procedure.

Scheme 2. Synthesis of 6-(2-(alkylamino)pyrimidin-5-yl) analogs 33-35*ᵃ*
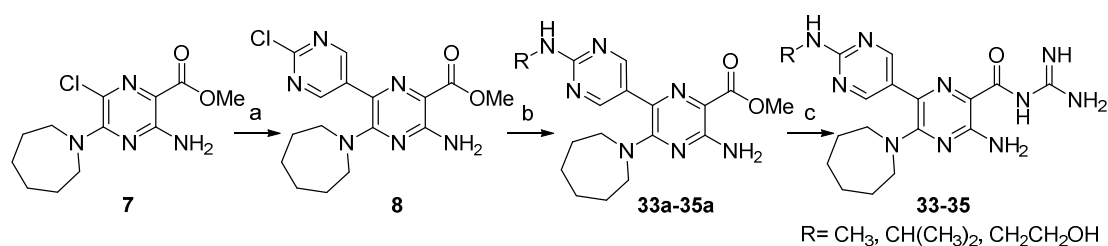
*a*Reagents and conditions: (a) (2-Chloropyrimidin-5-yl)boronic acid, Pd(PPh₃)₄, K₂CO₃, toluene/MeOH (4:1), reflux, 18 h, 64%; (b) (i) R-NH₂, DIPEA, DMF, rt, 2 d or (ii) R-NH₂, DIPEA, *i*-PrOH, reflux, 4 h, 83-87%; (c) guanidine (2 M in MeOH), DMF, rt, 18 h, 85-89%.

Previous reports describing napthamidine-based inhibitors[23-24] identified that the 2-aminopyrimidine group shows favorable binding in the uPA S₁β pocket. Based on this, 2-aminopyrimidinyl derivative **41** was synthesized using the route outlined in Scheme 3. The 3-

NH$_2$ group of methyl ester **7** was di-Boc protected using Boc-anhydride to give **36** in 85% yield. Halogen exchange from the 6-chloro group to 6-bromo in preparation for Buchwald-Hartwig amination was carried out over two steps. Hydrodechlorination using 1 atmosphere of hydrogen in the presence of Pd/C and MgO was successful, although it was accompanied by loss of one Boc-group giving mono-Boc derivative **37** in 92% yield. Introduction of the 6-bromo substituent using *N*-bromosuccinimide (NBS) gave **38** (60% yield) and Buchwald-Hartwig amination of **38** with 2-aminopyrimidine using Pd$_2$(dba)$_3$/Xantphos afforded the 6-substituted pyrazine methyl ester **39** in 30% yield. Removal of the remaining Boc-group with trifluoroacetic acid (98% yield) followed by guanidinylation delivered **41** (35% yield).

Scheme 3. Synthesis of 2-aminopyrimidinyl derivative 41[a]
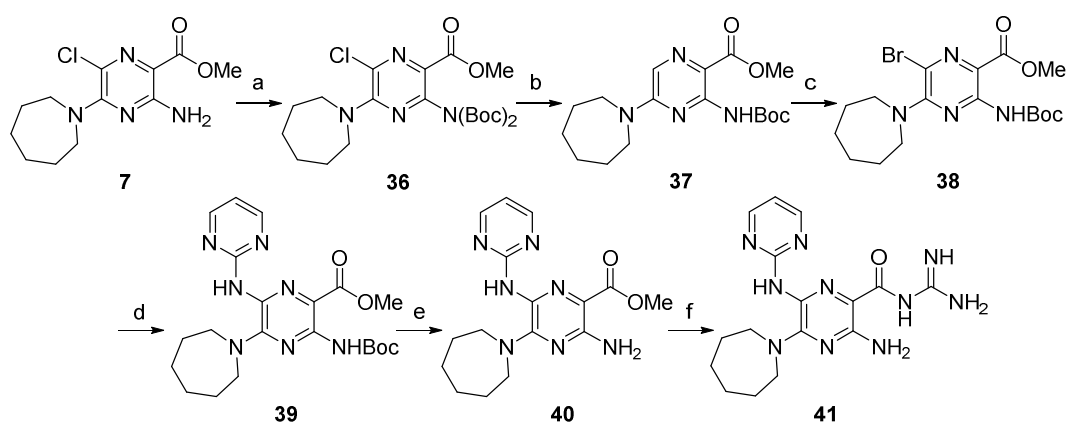
[a]Reagents and conditions: (a) (Boc)$_2$O, CH$_2$Cl$_2$, DIPEA, *N,N*-dimethylaminopyridine (DMAP), rt, 16 h, 85%; (b) Pd/C, H$_2$ (1 atm), MgO, MeOH, rt, 48 h, 92%; (c) *N*-bromosuccinimide, CH$_2$Cl$_2$, rt, 5 h, 60%; (d) 2-aminopyrimidine, Pd$_2$(dba)$_3$/Xantphos, 1,4-dioxane, Cs$_2$CO$_3$, 100 °C, 18 h, 30%; (e) TFA, CH$_2$Cl$_2$, rt, 16 h, 98%; (f) guanidine (2M in MeOH), DMF, rt, 35%.

Inhibition of uPA and structure-activity relationships. Inhibition of catalytically active, low molecular weight human uPA by **9-35** and **41** was determined using a fluorometric enzyme

activity assay.[53] Concentration-response curves for representative analogs **18** and **27** are provided in Figure 2 and calculated K_i values are presented in Table 1.
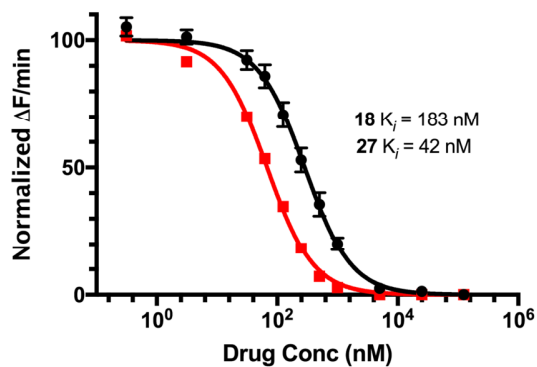
Figure 2. Inhibition of low molecular weight human uPA by **18** (black) and **27** (red). Data points represent the mean ± SEM (n = 3) from a single representative experiment.

Table 1. Inhibition of uPA by 6-substituted HMA analogs. For compounds where n >1, values represent the mean ± SEM from identical repeat assays conducted on different days. K_i were calculated from experimentally determined IC_{50}-values according to the methods of Cheng and Prussof[54].
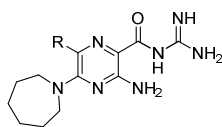
| Compound	R	uPA K_i (nM) [n]	Compound	R	uPA K_i (nM) [n]
4	amiloride	2433 ± 192 [1]	22		156 ± 20 [2]
5	HMA	1356 ± 183 [2]	23		166 ± 34 [2]
9		5020 ± 1750 [1]	24		1778 ± 249 [1]
10		16441 ± 1311 [1]	25		108 ± 17 [2]
11		4255 ± 194 [1]	26		53 ± 5 [2]
12		934 ± 151 [1]	27		42 ± 2 [4]
13		3539 ± 192 [2]	28		884 ± 14 [2]
14		508 ± 9 [2]	29		2198 ± 53 [2]
15		658 ± 66 [2]	30		1319 ± 310 [1]
16		5670 ± 1026 [1]	31		315 ± 34 [2]
17		3308 ± 300 [1]	32		21 ± 3 [2]
18		183 ± 10 [4]	33		43 ± 4 [2]
19		88 ± 33 [2]	34		42 ± 4 [2]
20		2417 ± 251 [1]	35		41 ± 2 [2]
21		1027 ± 170 [1]	41		228 ± 22 [2]

Amiloride **4** and HMA **5** returned K_i values of 2,433 nM and 1,356 nM, respectively, under the assay conditions. Replacing the 6-Cl group of HMA with a phenyl substituent **9** led to ~3.7-fold

decrease in potency. Substitution of the phenyl ring at the *para*-position (**10** and **11**) did not improve potency, while conversion to the 3,4-methylenedioxy derivative **12** provided a slight increase relative to HMA (K_i= 934 nM). Appending an isoquinolyl group **13** reduced activity nearly 3-fold relative to HMA. *N*-methylpyrazole derivative **14** showed a ~ 2.7-fold increase(K_i= 508 nM). Extension of the *N*-methyl group of **14** to *N*-ethylmorpholino **15** had only a minor effect (K_i = 658 nM). Surprisingly, while 2-indolyl **16** and 2-benzothiophenyl substituents **17** showed reduced activity, the single atom change to 2-benzofuranyl derivative **18** afforded a significant boost in potency (K_i = 183 nM), which increased 2-fold upon addition of a fluorine atom at the benzofuran 4-position (**19**, K_i = 88 nM). The preference for oxygen in the heteroaryl ring was also seen with the 2- and 3-furanyl derivatives **22** and **23**, respectively, which both showed nM potency whereas 2- and 3-thiophene derivatives **20** and **21** were micromolar inhibitors.

2-Fluoropyridine substitution (**24** K_i = 1,778 nM) afforded similar activity to HMA **5**, while addition of a 5-pyrimidinyl group **25** (K_i = 108 nM) gave a ~12.6-fold increase. Addition of a methoxy group to the pyrimidine 2-position yielded the first sub-100 nM inhibitor **26** (K_i = 53 nM), and adding a second methoxy group to the pyrimidine 4-position **27** (K_i = 42 nM) gave a further increase. The favorable binding of the pyrimidine group was evident from the significant losses in potency observed with dimethoxypyridine **28** and dimethoxyphenyl derivatives **29** and **30**. Loss of potency with the dimethoxypyridazine **31** was less dramatic (K_i = 315 nM). An additional 2-fold gain in potency was achieved upon addition of an amine to the pyrimidine 2-position, yielding the most potent inhibitor in the study (**32** K_i = 21 nM). Further gains in potency were not obtained through *N*-alkyl substitution, with *N*-methyl **33**, *N*-isopropyl **34** and

N-hydroxyethyl **35** derivatives showing activity similar to **26**. The 2-aminopyrimidine derivative **41** obtained using Buchwald-Hartwig chemistry showed lower potency (K_i = 228 nM).

X-ray crystallography. An X-ray co-crystal structure was obtained for HMA **5** bound to the catalytic domain of human uPA (Figure 3). The binding orientation and interactions observed in the HMA:uPA structure mirrored those previously observed with amiloride **4**.[51] The key salt bridge interaction was present between the acylguanidine of HMA and the Asp189 side chain carboxylate located at the base of the S1 binding pocket. H-bonds were present between the backbone carbonyl of Gly219 and the terminal NH and amide NH groups of the acyl guanidine. The second terminal guanidine-NH formed an H-bond to the side chain hydroxyl of Ser190 and the exocyclic NH_2 group at C3 formed an H-bond to the side chain hydroxyl of Ser195. A bridging H-bond network was observed between a surface-bound water molecule, the acyl guanidine carbonyl oxygen, Ser190 side chain hydroxyl and a guanidine NH group. A sulfate ion from the crystallization buffer was observed in the oxyanion hole of both structures.
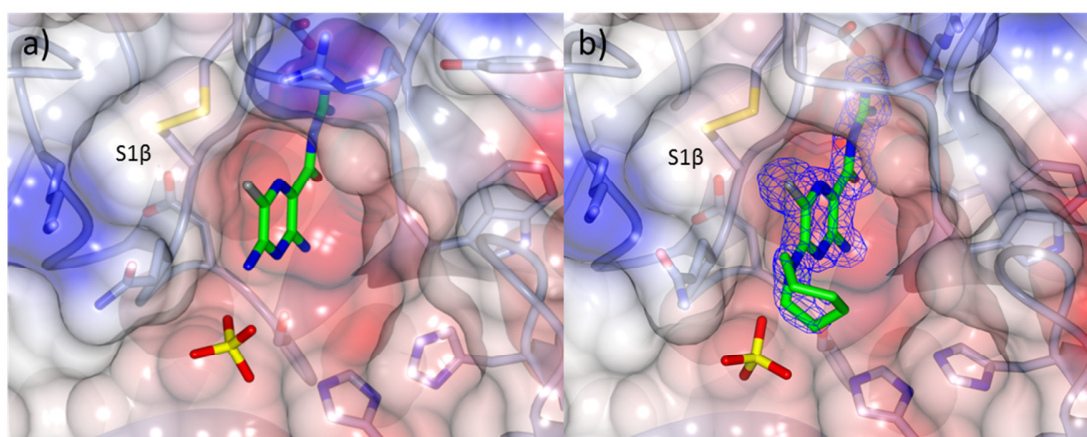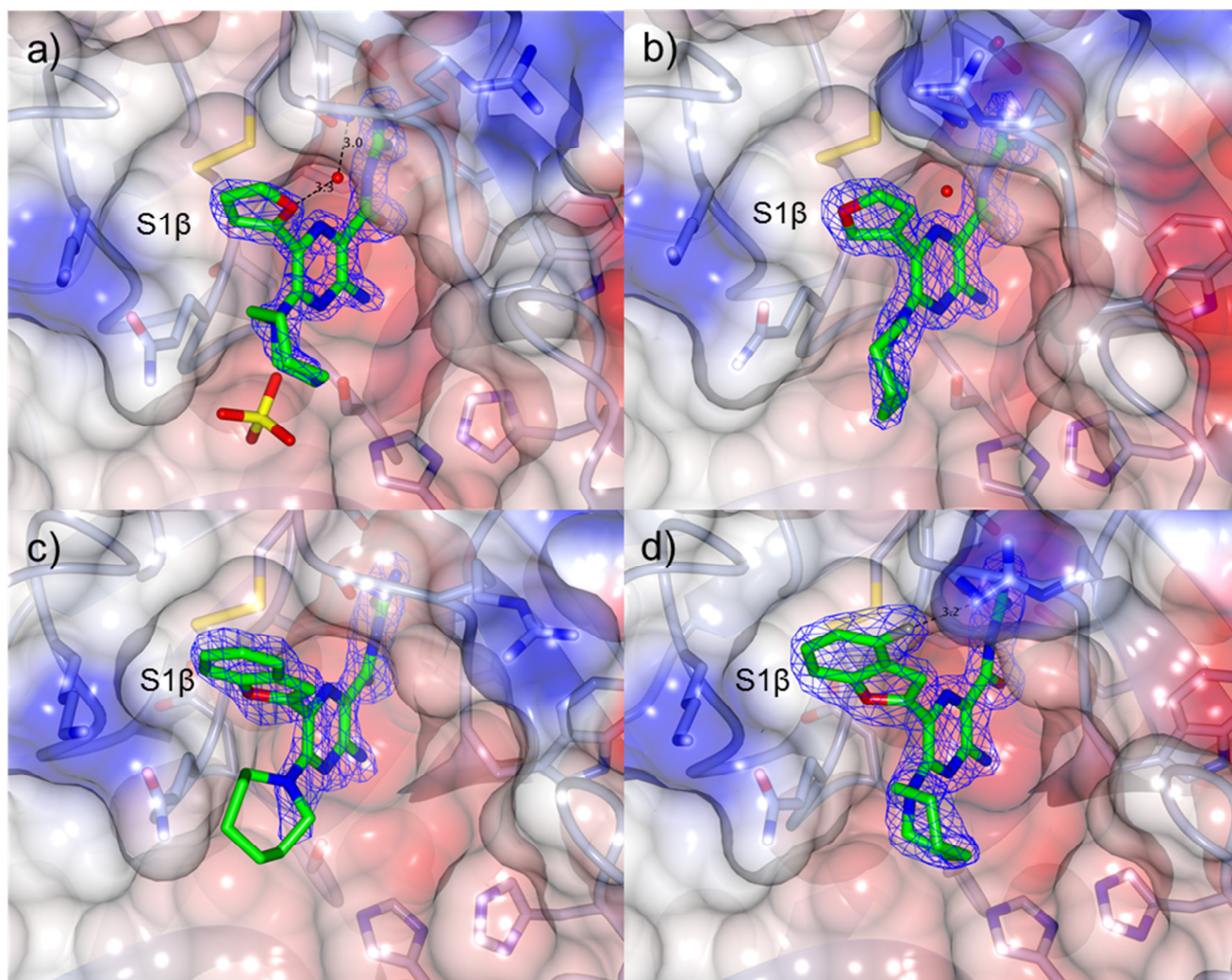

Figure 3. X-ray co-crystal structures of (a) amiloride **4**[51] *(PDB ID: 1F5L)* and (b) HMA **5** *(PDB ID: 5ZA7*, 1.7 Å resolution) bound to uPA. Blue wire basket = $2mF_o$-DF_C map contoured at 1.5 σ.

X-ray co-crystal structures were similarly obtained for benzofuran (**18**, **19**), furan (**22**, **23**), pyrimidine **25**, 2-methoxypyrimidine **26**, 2,4-dimethoxypyrimidine **27** and *N*-methylpyrazole **14** analogs (Figures 4 and 5. X-ray refinement statistics are provided in Supporting Information, Table S1). H-bonding networks reminiscent of those seen in the HMA:uPA structure were observed in all complexes. The 7-membered hexamethylene ring appeared to sample multiple conformations, as evidenced by low electron density in all structures. Replacement of the 6-Cl group with (hetero)aryl substituents did not significantly alter the binding positions or orientation of the pyrazine core or acylguanidines relative to HMA **5**. The 6-substituent occupied S1β in all cases and sulfate ion occupied the oxyanion hole in some complexes.

The structure obtained with 2-furanyl analog **22** (Figure 4a) revealed that the ~8.7-fold increase in potency relative to HMA **5** may arise from new H-bonds formed between the furanyl O, a bridging water molecule and the amide NH of Gly219. Favorable van der Waals contacts between the furan ring and Gly219, the Cys191-Cys220 disulfide, Ser146 backbone carbonyl and the side chain Cβ and Cγ of Gln192 were also apparent. Changing to the 3-furanyl substituent **23** had little effect on uPA activity despite the furanyl oxygen no longer making the water-bridged H-bond interaction with Gly219 (Figure 4b). Flexibility of the Arg217 side chain was noted in this structure, where it had shifted towards S1β to participate in the Gly219-bridging water H-bond network. Relative to **22**, the plane of the furan ring in **23** was tilted 11˚, a pose that promoted van der Waals interactions with Cys220. Interactions with S1β residues Cys191-Cys220, Ser146 and the Gln192 side chain were preserved and there appeared to be a dipolar interaction between the side chain carbonyl of Gln192 and the polarized furan 2-CH group.

Ring fusion to give benzofuran **18** led to a slight decrease in potency ($K_i = 183$ nM) relative to **22** despite this group extending further into S1β and almost completely occupying the subsite (Figure 4c). The plane of the benzofuran ring was essentially perpendicular to the pyrazine core but the ring oxygen had flipped 180° relative to the furanyl oxygen of **22**. This orientation allowed the benzofuran 7-CH group to fill a small, hydrophobic dimple formed by Lys143, Gln192 and Ser146. Additional hydrophobic contacts were seen between the benzofuran 3- and 4-position CH groups and Gly219. Similar to what was observed in the HMA **5** and **22** structures, the side chain of Arg217 adopted a conformation well away from S1β. The structure with **19** suggested that the 2-fold increase in potency obtained after fluorine substitution at the benzofuran 4-position (**19** $K_i = 88$ nM) arose from favorable interactions between the 4-fluoro group and the side chain guanidine of Arg217 (possibly an H-bond), which had shifted back towards S1β in this complex. The interaction with Arg217 also appeared to cause a slight twisting about the benzofuran-pyrazine axis away from perpendicular, with the 78° dihedral angle in **18** reducing to 68° in **19**.

Figure 4. X-ray co-crystal structures of: (a) **22** (PDB ID: 5ZAE, 1.7Å), (b) **23** (PDB ID: 5ZAF, 1.7Å), (c) **18** (PDB ID: 5ZA9, 1.6Å) and (d) **19** (PDB ID: 5ZC5, 1.9Å) bound to uPA. Blue wire baskets represent $2mF_o$-DF_C maps contoured at 1.5 σ.

The 5-pyrimidine substituent of **25** was found to partially occupy S1β (Figure 5a), making van der Waals interactions with the Cys191-Cys220 disulfide, Ser146 and Gln192 residues. A dipole interaction between the polarized 4-CH group of the pyrimidine and the Gln192 side chain carbonyl appeared to be present, along with an H-bond between the amide NH of Gly219 and the lone pair of electrons on a pyrimidine nitrogen. The polarized 6-CH on the pyrimidine appeared to interact with the Gly219 carbonyl group.

Addition of a methoxy group to the pyrimidine 2-position **26** led to a ~ 2-fold increase in potency, but it did not appear to make any specific interactions with the protein, instead orienting towards bulk solvent (Figure 5b). The sidechain of Arg217 had flipped back towards S1β driven by a polar interaction with the pyrimidine nitrogen (possibly an H-bond).

Introduction of a second methoxy substituent onto the pyrimidine ring **27** resulted in a small increase in potency relative to **26**. The pyrimidine and pyrazine rings were almost perpendicular (dihedral angle 80°), allowing for increased occupancy of S1β and projection of a methoxy group towards the small hydrophobic dimple formed by Lys143, Gln192 and Ser146 (Figure 5c). The second methoxy substituent was projected towards bulk solvent. In contrast to **25** and **26**, the Arg217 side chain was positioned well away from S1β, apparently to avoid a steric clash with the pyrimidine 2-OCH_3 group of **27**.

The *N*-methylpyrazole substituent of **14** adopted a coplanar arrangement with the pyrazine reducing its penetration into S1β (Figure 5d). Interactions were observed between the pyrazole 3-CH and 5-CH groups and the backbone of Gly219 and the side chain of Gln192, respectively. The surface water molecule bound to Gly219 in the furanyl structures **22** and **23** was observed but did not appear to interact with the pyrazole.
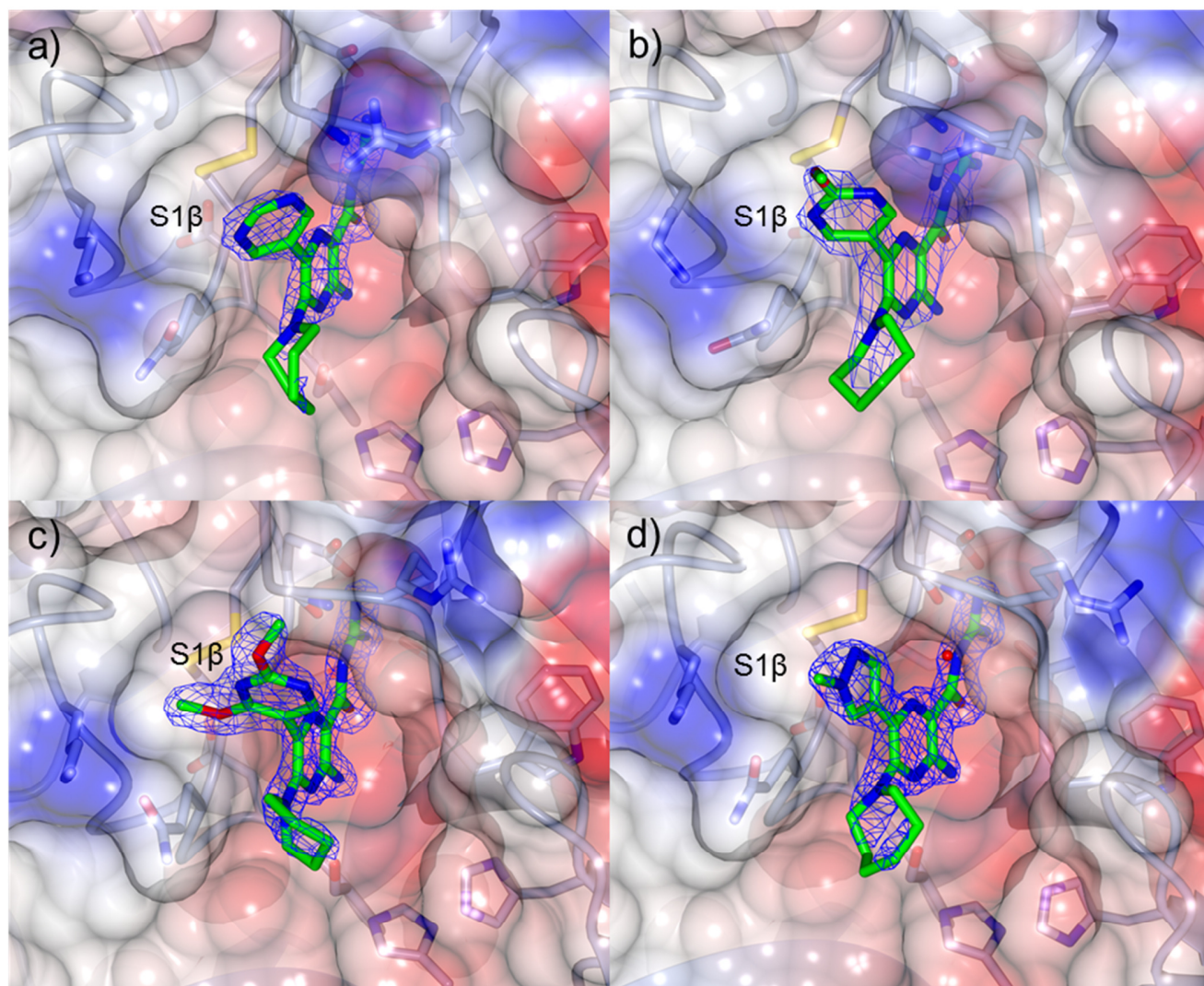
Figure 5. X-ray co-crystal structures of: (a) **25** (PDB ID: 5ZAG, 2.0 Å), (b) **26** (PDB ID: 5ZAH, 3.0 Å), (c) **27** (PDB ID: 5ZAJ, 1.7 Å) and (d) **14** (PDB ID: 5ZA8, 1.9 Å) bound to uPA. Blue wire baskets represent $2mF_o$-DF_C maps contoured at 1.5 σ.

Inhibition of trypsin-like serine proteases. HMA **5** and 6-substituted analogs **18**, **19** and **26** were screened against a panel of trypsin-like serine proteases (TLSPs) using chromogenic assays (Table 2). Comparable uPA inhibition was observed with the four compounds under chromogenic (Table 1) and fluorometric (Table 2) assay conditions. In agreement with earlier

reports showing that occupancy of uPA's S1β subsite confers high selectivity over other TLSPs,[20, 23, 55] each of the compounds showed 20-100+ fold selectivity for uPA.

Table 2. uPA selectivity versus related trypsin-like serine proteases of HMA **5** and 6-substituted analogs **18**, **19** and **26**. Values were obtained using chromogenic enzyme inhibition assays.[40] N/D = not determined.

		IC$_{50}$ (µM)								
Compound	R	uPA	tPA	Plasmin	Thrombin	Trypsin	Human plasma kallikrein	Factor Xa	Factor XIa	Activated protein C
5	Cl	2.4	>10	>10	>10	>10	>50	>50	>50	>50
18		0.53	>10	>10	>10	>10	11.3	>50	31.0	>50
19	F	0.43	>20	>20	>20	N/D	16.7	>50	23.3	>50
26	MeO	0.039	>20	>20	>20	N/D	>50	>50	>50	>50

To further probe uPA selectivity, super-family wide screening against 85 serine hydrolases was performed *in-situ* using the recently described EnPlex activity-based protein profiling (ABPP) assay[56]. In this approach, individual serine hydrolases are conjugated to differently colored Luminex beads and the ability of inhibitory compounds to outcompete a biotinylated serine-reactive/SAPE probe at the active site of each enzyme provides a rapid and semi-

quantitative readout of enzyme inhibition. Results from the Enplex screen with amiloride **4**, HMA **5** and 6-substituted analogs **18**, **25** and **26** are shown in Figure 6.

Figure 6. EnPlex[56] screening of amiloride **4**, HMA **5** and analogs **18**, **25** and **26** for inhibition of 85 serine hydrolases. Grey boxes indicate wells in which no fluorescence was observed. The singular readouts suggesting activity of **4** and **26** against LIPE are artifacts. Black arrows indicate decreasing compound concentration from 33.3 μM to 10 nM.

Amiloride showed slight activity against only a few serine hydrolases (*C1R*,*C1S*, *DDHD1*, Factor VIIa and *LACTB*), consistent with its reported high selectivity for uPA.[37] HMA **5** showed activity against the highly homologous S28 protease family members dipeptidyl peptidase 2 (*DPP7*) and prolylcarboxypeptidase (*PRCP*).[57] Surprisingly, inhibitory activity against uPA was not observed for HMA under these assay conditions. 2-Benzofuranyl analog **18** showed the least selectivity among the tested compounds, inhibiting plasma kallikrein (*KLKb1*) and trypsin. 5-Pyrimidinyl analog **25** showed remarkable selectivity for uPA, with slight inhibition of trypsin being the only off-target TLSP activity observed. 2-Methoxy pyrimidinyl analog **26** showed slight activity against *C1S*, plasma kallikrein, plasmin, prolylcarboxy peptidase, trypsin and transmembrane protease serine 11D (*TMPRSS11d*).

Human cell cytotoxicity. HMA **5** and representative analogs **18**, **19**, **25** and **26** were tested for cytotoxicity against four human cell lines (Table 3). HMA **5** showed toxicity in the low micromolar range against all cell lines, with HEK-293 embryonic kidney and HT-1080 fibrosarcoma cells being most sensitive. In general, the cell lines were more sensitive to **18**, suggesting the benzofuran group may contribute to cytotoxic effects. MDA-MB-231 cells were ~3-fold more sensitive to the 4-fluorinated benzofuran **19** but the compound was less toxic than **18** towards the other three cell types. Cytotoxicity was not a general feature of 6-substituted HMA analogs since pyrimidine analogs **25** and **26** showed much lower activity against all cells. The lower $logD_{7.4}$ of the pyrimidines (i.e. 2.8 and 3.4, respectively) relative to benzofuran **18** (i.e. $logD_{7.4}$ 5.1) and HMA ($logD_{7.4}$ 3.8) suggests lipophilicity may be a contributor to cytotoxicity.

Table 3. Effect of HMA and selected analogs on human cell viability.

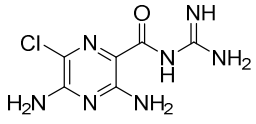| Compound	R	MDA-MB-231 IC$_{50}$ (μM)	HepG2 IC$_{50}$ (μM)	HEK-293 IC$_{50}$ (μM)	HT-1080 IC$_{50}$ (μM)
5		27.3	20.2	2.8	6.6
18		10.9	12.7	3.1	4.6
19		3.2	68.4	12.0	2.1
25		>100	>100	>100	37.1
26		>100	57.3	74.9	44.8
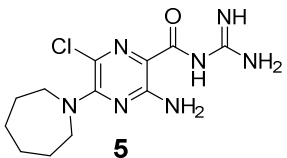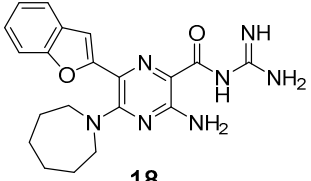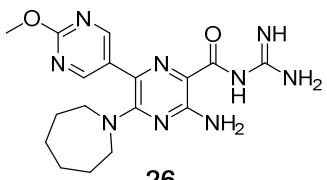
Off-target activity against GPCRs. Amiloride and related analogs are known to bind to G-protein coupled receptors (GPCRs).[58-59] For example, amiloride is a known antagonist of the adenosine 2A receptor (A$_{2A}$).[60-62] Recent work describing the effects of substitution at the amiloride 5-position on A$_{2A}$ antagonism identified analogs with increased potency, including HMA **5**.[63] In the current study, a representative selection of 6-substituted HMA analogs were evaluated alongside HMA **5** for A$_{2A}$ antagonism using a radiolabeled ligand displacement assay (Figure 7). In all cases, the presence of the 6-substituent diminished antagonist effects relative to HMA, with the majority of compounds showing poor A$_{2A}$ binding.
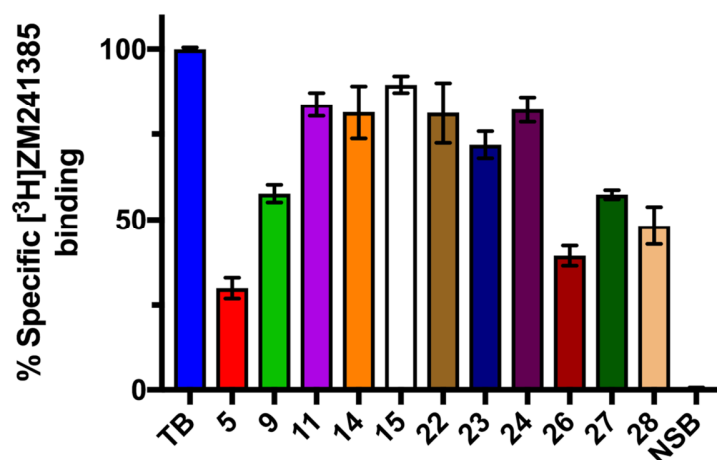
Figure 7. Single concentration screening (10 µM) of HMA **5** and 6-substituted HMA analogs as antagonists of the human adenosine A_{2A} receptor ($hA_{2A}AR$-WT). Radioligand [³H]ZM241385 was present at 2.5 nM. Total binding (TB, 100%) of [³H]ZM241385 was determined in the absence of inhibitors. Non-specific binding (NSB, 0%) was determined in the presence of 100 µM A_{2A} agonist 5'-(*N*-ethylcarboxamido)adenosine (NECA). Data represent the mean ± SEM from at least three independent experiments conducted in duplicate. Methods were as described in reference [63].

Development of active site-directed uPA inhibitors has been complicated by the observation that compounds optimized for high affinity against human uPA often show reduced potency against the homologous mouse enzyme.[64] This species selectivity can confound interpretation of data from mouse models as the decreased affinity for mouse uPA may lead to an underestimation of compound efficacy. To explore this issue in the 6-substituted HMA class, we measured the activities of **4**, **5**, **18** and **26** against mouse uPA (Table 4).

Table 4. Activity of compounds **4**, **5**, **18** and **26** against human and mouse uPA. [a]Experimental replicates were performed as described in Table 1.[b]Value is the average of two independent experiments.

Compound	Human uPA K_i (nM)[a]	Mouse uPA K_i (nM)[b]	Human/Mouse Selectivity Ratio
4	2,433	2,313	0.95
5	1,356	9,308	6.86
18	183	1,802	9.85
26	53	1,611	30.40

Amiloride **4** was essentially equipotent against mouse and human uPA. Addition of the 5-hexamethylene ring in **5** decreased affinity for mouse uPA by almost 7-fold, while compounds **18** and **26** showed larger (10- to 30-fold) reductions. These findings align with reported trends for compounds bearing substituents that target uPA's S1β subsite.[64] The lower potency against mouse uPA was a key consideration in dose selection for *in vivo* studies with **18** and **26** (see below).

Diuretic and anti-kaliuretic effects. The potassium-sparing activity of amiloride arises from inhibition of epithelial sodium channels (ENaCs) in the kidneys, leading to reduced urinary excretion of K^+.[34] In cases of overdose, the potassium-sparing effects can lead to hyperkalemia and cardiac arrhythmias.[65] As such, removal of ENaC activity is essential for development of a 6-substituted HMA analog suitable for use in cancer. Early work from the Cragoe group at Merck established that alkyl substitution of the 5-NH_2 group of amiloride reduces ENaC activity,[49] and showed that HMA produces >80-fold lower inhibition than amiloride in a deoxycorticosterone acetate (DOCA) induced K^+ excretion model in adrenalectomized rats.[49] 6-Substituted HMA analogs were thus expected to show similarly low activity against ENaCs. To confirm this, a representative selection of analogs was tested against recombinant HEK-293 cells that overexpress the α, β and γ subunits of human ENaCs (Figure 8). In line with expectations, amiloride **4** produced a strong effect (68% inhibition of ENaC at 10 µM), whereas HMA **5** showed greatly reduced activity and 6-substituted analogs **11**, **18**, **25** and **26** showed similar or lower inhibition than HMA.
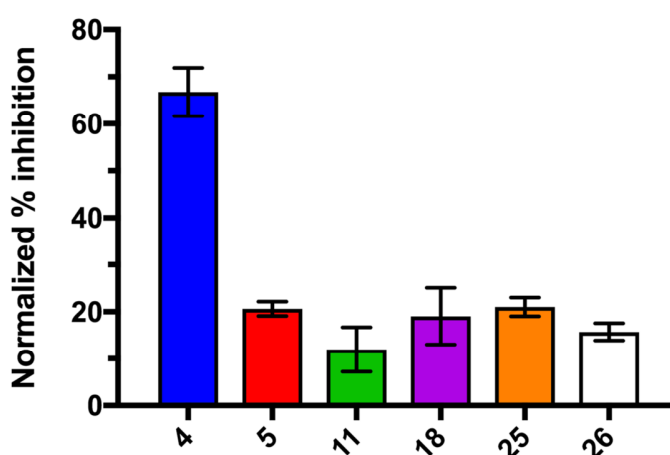
Figure 8. Inhibition of ENaC activity by amiloride **4**, HMA **5** and 6-substituted analogs **11**, **18**, **25** and **26** in transfected HEK-293 cells. All compounds were present at 10 µM. Data represent the mean ± SD (n = 4).

Amiloride **4**, HMA **5** and analogs **18** and **26** were next tested in a rat model of diuresis to confirm that loss of ENaC inhibitory potency corresponded to an absence of diuretic and anti-kaliuretic effects *in vivo* (Figure 9). With the exception of vehicle controls, all animals were dosed with 25 mg/kg acetazolamide to induce diuresis[66] prior to receiving 1.5 mg/kg of amiloride **4**, HMA **5**, **18** or **26**. Urine was collected over a 6 h period following dosing. Consistent with previous reports, amiloride **4** showed potent diuretic and anti-kaliuretic effects, increasing urine volume and sodium excretion by 34% and 159% respectively, while decreasing potassium excretion by 92% relative to acetazolamide-treated controls (Na^+/K^+ excretion ratio = 63, p <0.0001 for all measurements).[66] Compound **18** did not significantly decrease K^+ excretion, while HMA **5** and 2-methoxypyrimidine analog **26** showed a very slight potassium-sparing effect (24% reduction, p <0.001). HMA **5**, **18** and **26** did not alter Na^+ excretion or urine volume and the Na^+/K^+ excretion ratios for the three compounds were no different to acetazolamide treated controls (range = 2.44-2.68).

K⁺ Excretion — **Na⁺ Excretion** — **Urine Flow** — **Na⁺/K⁺ Excretion Ratio**
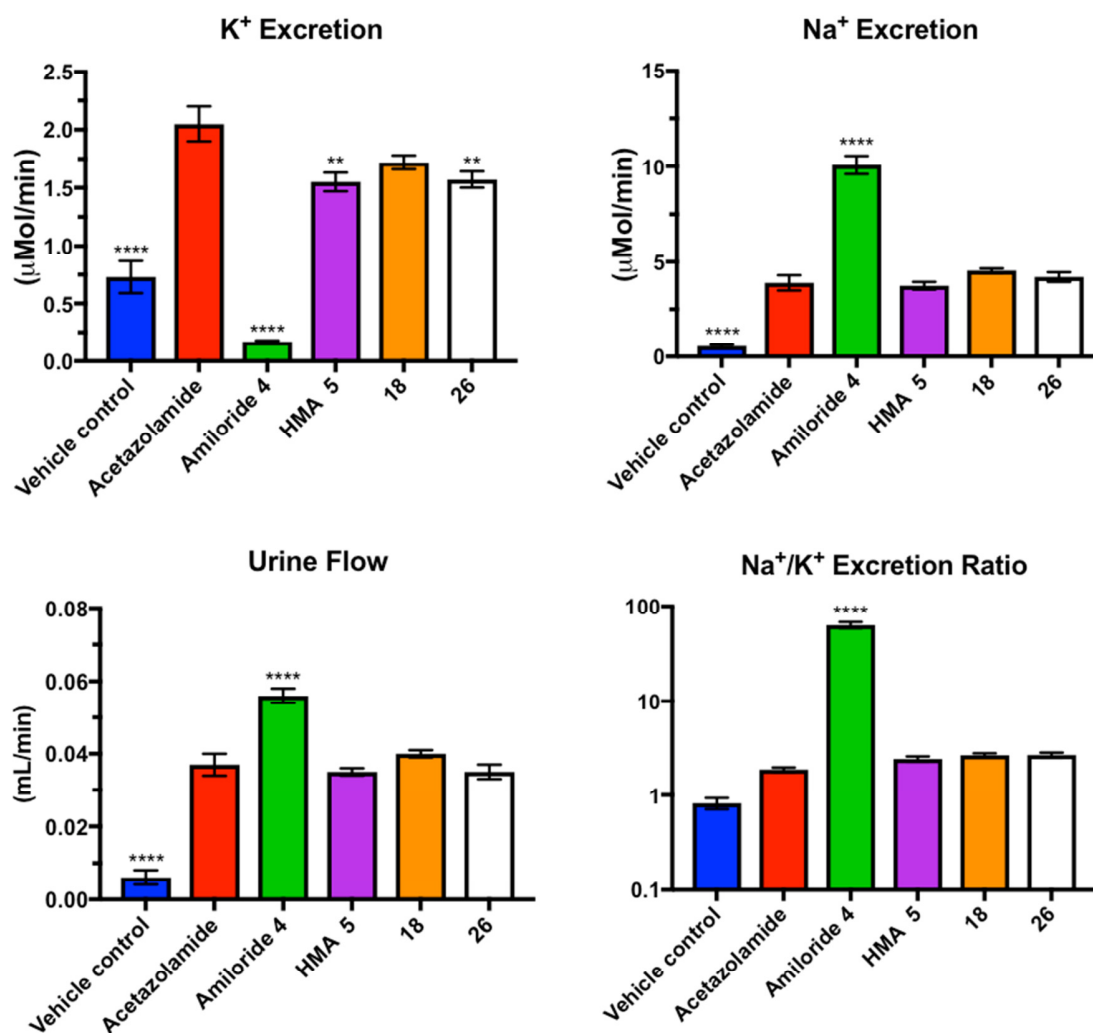
Figure 9. Effects of amiloride **4**, HMA **5** and 6-substituted analogs **18** and **26** on urine flow and excretion of Na^+ and K^+ in Sprague Dawley rats. Rats were dosed with 25 mg/kg acetazolamide prior to administering 1.5 mg/kg of test compound. Data represent the mean ± SEM (n = 8). ** = $p < 0.001$, **** = $p < 0.0001$ relative to acetazolamide control.

Experimental lung metastasis model. Two analogs were advanced to anti-cancer pilot studies to establish efficacy *in-vivo*. Compounds **18** and **26** were selected as representative examples showing different potency and polarity (**18** $logD_{7.4}$ = 5.1, **26** $logD_{7.4}$ = 3.4). In the first study, amiloride **4** and 6-substituted HMA analogs **18** and **26** were examined for anti-metastasis effects

in an experimental mouse model of late-stage lung metastasis. Luciferase-tagged HT-1080 human fibrosarcoma cells were used in the model after confirming cell surface expression of uPA/uPAR (Supporting Information Figure S1). Assays of lung homogenates following organ harvest at endpoint were used to quantitate lung tumor burden and response to treatment. Animals received 2.5×10^5 HT-1080 cells via lateral tail vein injection on Day 0 and were weighed and scored for clinical signs (scoresheet Supporting information Figure S2) over 21 days. Animals received 7.5 mg/kg/day of compound (or vehicle) via IP injection from Day -1 to Day 20. This dose was selected based on extensive *in vivo* pharmacokinetic profiling and represented a compromise between tolerability and attempting to demonstrate efficacy with compounds that show reduced potency against murine uPA.[67]
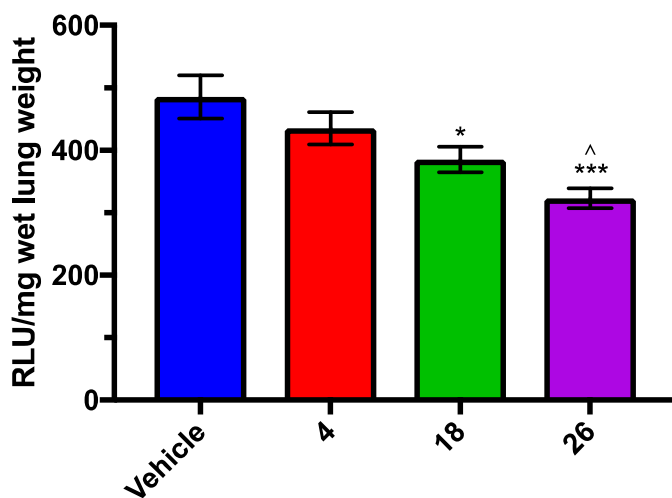
Figure 10. Effects of amiloride **4**, **18** and **26** in experimental mouse model of late-stage lung metastasis. All compounds were administered once daily at 7.5 mg/kg/day for 21 days. Lung metastasis was quantified by endpoint luciferase assay of lung homogenates. Data represent the mean ± SEM (**18** and **26** n = 6; Vehicle and **4** n = 4). * = p <0.03; *** = p <0.001 relative to vehicle control, ^ = p <0.03 relative to **4**.

Amiloride **4** did not significantly inhibit metastasis in this model at the concentration tested. Benzofuranyl analog **18** decreased metastasis by 21% (p = 0.0297) relative to control but there was no statistically significant difference between amiloride and **18** (Figure 10). 2-Methoxy pyrimidine analog **26** significantly decreased lung metastasis (33%, p = 0.0007).

Orthotopic model of pancreatic cancer. The *in vivo* anti-tumor and anti-metastasis effects of **18** and **26** were evaluated alongside the standard of care drug gemcitabine in an orthotopic xenograft mouse model of pancreatic cancer (Figure 11). Briefly, female athymic nude mice (BALBc nu/nu, 8-11 weeks of age) were anaesthetized and an incision was made in the left flank and the spleen and tail of the pancreas were externalized. A mixture of human pancreatic cancer cells (AsPC-1) 1×10^6 and human pancreatic stellate cells (hPSCs) 1×10^6 in 50µL PBS was injected into the tail of the pancreas. uPA expression was confirmed in both cell lines by Western Blot analysis (Supporting Information Figure S3).[68] The pancreas and spleen were then reinternalized and the wound closed. Seven days after cell implantation, mice were randomized to receive treatment with gemcitabine (75 mg/kg PO twice weekly), **18** or **26** (10 mg/kg IP daily) for 28 days (n = 4 mice/group). The higher dose (relative to the lung metastasis model) was chosen to increase the likelihood of observing efficacy. In line with previous observations in this model, Gemcitabine showed only modest inhibitory effects on the primary tumour.[69] Measurement of tumor volume at endpoint revealed that **18** and **26** produced similar reductions to gemcitabine on the primary mass (Figure 11A). Notably, liver metastases (key site in this model) were reduced in mice treated with compounds **18** and **26** compared to those treated with gemcitabine, with no macroscopic metastatic lesions observed in any mice that received **26**

(Figure 11B). The absence of liver metastases in all animals treated with **26** was confirmed by histology (Supporting Information Figure S4).
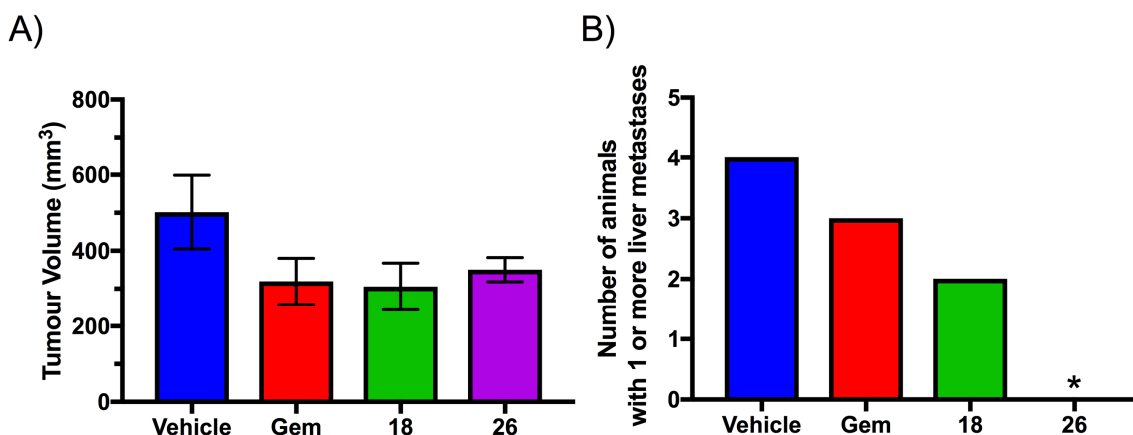
Figure 11. A) Effects of gemcitabine (Gem), **18** and **26** on endpoint primary tumor volume in an orthotopic xenograft pancreatic cancer model. Mice received oral gemcitabine 75 mg/kg twice weekly or daily intraperitoneal injections of **18** or **26** (10 mg/kg) for 28 days. Data represent the mean ± SEM (n = 4 per group). B) Number of mice with histologically confirmed liver metastases after receiving gemcitabine, **18** and **26** (n = 4 per group). *p = 0.0285 vs Vehicle, Chi-square test.

CONCLUSIONS

This study reveals that 6-substituted HMA derivatives are potent inhibitors of human uPA with potential for development into a new class of anti-cancer drugs. Access to a diverse series of 6-(hetero)aryl analogs was afforded via a simple two step Suzuki-Miyaura/acyl guanidinylation approach using commercial boronic acids/esters and a common 6-chloropyrazine intermediate **7**. The key intermediate was easily synthesized on multigram scale in a single step

from commercial reagents. Buchwald-Hartwig chemistry was established on a related 6-bromopyrazine scaffold to access 6-aminopyrimidine HMA derivative **41**. Given the general reactivity of halopyrazines in transition metal-catalyzed cross-coupling reactions,[70] it is likely that a great many other substituents could be appended at the 6-position of HMA using this chemistry. Screening of such a library against proteins that reportedly bind to HMA (e.g. P2X$_7$[71], NHE1[72], HIV-1 Vpu[73], Influenza A M2[74], GnRHR[75], GABA-A ρ-1[76], ASIC1a[77] and GIRK) could help to identify more potent and selective probes for these targets, and possibly therapeutic leads.

Leading compounds from the study showed uPA inhibitory potencies more than 10-fold higher than HMA, with X-ray crystallography revealing that the gains arose from interactions formed between the appended 6-substituents and uPA's S1β pocket. High target selectivity was demonstrated across the serine hydrolase superfamily and selected analogs showed no activity against ENaCs *in vitro* or K$^+$-sparing/diuretic effects *in vivo*. Analogs carrying 2-benzofuranyl and 5-pyrimidinyl substituents emerged as distinct lead classes with differing physicochemical properties and human cell cytotoxicity profiles. Examples from each class were found to inhibit formation of lung metastases in a mouse experimental metastasis model, and 2-methoxypyrimidine analog **26** completely inhibited formation of liver macrometastases in a mouse pancreatic cancer model. In summary, this work reports the successful repurposing of the diuretic amiloride into potent uPA inhibitors with attractive pharmacological properties for further evaluation as a novel class as anti-cancer agents for treating uPA-driven malignancies.

Experimental

Chemistry – General. All solvents and chemicals were purchased and used without further purification except ^{i}PrOH, which was distilled from BaO and stored over 4 Å molecular sieves

under Ar. Progress of reactions was monitored using Merck silica gel 60 F_{254} TLC plates with EtOAc/Pet.spirit mixtures as eluent. Compound spots on TLC plates were visualized under UV light at 254 nm. Column chromatography was performed using Merck silica gel 60 (230-400 mesh). Melting points (mp) were measured in open capillaries using a Griffin Analog Melting Point Apparatus (Thermo-Fisher Scientific, Waltham, Massachusetts, USA) and are uncorrected. ^{1}H and ^{13}C NMR spectra were recorded using a Varian Inova 500 or Varian Premium Shielded 500 (499.74 MHz for ^{1}H; 125.66 MHz for ^{13}C) in deuterated solvents. Chemical shifts are reported in parts per million (δ ppm) relative to TMS for ^{1}H or the solvent peak for ^{13}C. High-resolution mass spectrometry (HRMS) analysis was performed using a Waters XEVO QToF mass spectrometer (Waters Corporation, Milford, Massachusetts, USA) with leucine encephalin as internal standard. Purity of all final compounds was confirmed at > 95% using high performance liquid chromatography (HPLC). HPLC analyses were performed using a Shimadzu CLASS-VP LC10 Analytical HPLC system (Shimadzu Corporation, Kyoto, Japan) with detection at 254 nm. Gradient elutions were performed using mixtures of solvent 100% H_2O/0.1% TFA and 100% CH_3CN/0.1% TFA on a Waters VisionHT 3 µm C18 column (150 mm x 4.6 mm) at a flow rate of 0.5 mL.min^{-1}. Column temperature was not controlled. Only one previous 6-substituted HMA analog (6-phenyl HMA) has been reported but no characterization or uPA inhibition data were described.[78]

Chemistry – Experimental procedures and compound characterization

Synthesis of methyl 3-amino-6-chloro-5-hexamethyleneimine-2-pyrazinecarboxylate (7).

To a suspension of methyl 3-amino-5,6-dichloro-2-pyrazinecarboxylate (5.55 g, 25.0 mmol) in 2-propanol (50 mL) was added hexamethyleneimine (2.73 g, 3.10 mL, 27.5 mmol). Diisopropylethylamine (3.55 g, 4.79 mL, 27.5 mmol) was added and the reaction mixture was heated at reflux for 2 hours. The reaction mixture was allowed to cool to room temperature, which caused the product to crystallize. The solid product was collected by vacuum filtration and washed with cold 2-propanol (2 x 10 mL) and then diethyl ether (10 mL). After drying, the pure product was obtained as pink crystals (6.1 g, 86%). mp 109-111 °C; ^{1}H NMR (CDCl$_3$): δ 6.13 (br s, 2H), 3.89 (s, 3H), 3.82 (t, *J* = 6.0 Hz, 4H), 1.84 (s, 4H), 1.58 (s, 4H); ^{13}C NMR (CDCl$_3$): δ 166.4, 153.7, 153.1, 120.3, 111.3, 52.0, 51.1, 28.4, 26.7; MS (ESI): *m/z* 285 (M+H)$^+$, 307 (M+Na)$^+$; HRMS (ESI$^+$) Anal. for C$_{12}$H$_{17}$N$_4$NaO$_2$$^+$: Calc. mass 307.0932, found 307.0938.

General Method A: Suzuki-Miyaura coupling reactions

Methyl 3-amino-6-chloro-5-hexamethyleneimine-2-pyrazinecarboxylate **7** (1 eq.) was combined with K$_2$CO$_3$ (10 eq.), the appropriate boronic acid (1.5 eq.) and Pd(PPh$_3$)$_4$ (5 mol%) in a two-neck round bottom flask. The flask was connected to a condenser and purged with nitrogen. A 4:1 dry toluene: MeOH mixture (60 mL) was added via syringe and the reaction mixture was heated at reflux for 0.5-18 h. The mixture was allowed to cool to room temperature and filtered through Celite (10 x 3 cm, eluting with 3 x 20 mL EtOAc). The filtrate was evaporated to dryness and the residue purified by silica gel flash column chromatography using EtOAc/pet spirit.

Methyl 3-amino-5-(azepan-1-yl)-6-(4-(methylthio)phenyl)pyrazine-2-carboxylate (10a)

General Method A using 4-(methylthio)phenyl boronic acid (93 mg, 0.545 mmol) afforded

10a as a yellow solid; yield 77% (104 mg, 0.279 mmol); MP: 132-134 °C; ^{1}H NMR (500 MHz,

CDCl$_3$) δ 7.42 (d, J = 8.1 Hz, 2H), 7.25 (d, J = 8.1 Hz, 2H), 6.20 (bs, 2H), 3.88 (s, 3H), 3.36 (t, *J*

= 5.5 Hz, 4H,), 2.48 (s, 3H), 1.62 (s, 4H), 1.43 (s, 4H); ^{13}C NMR (126 MHz, CDCl3) δ 167.4,

154.8, 153.4, 137.8, 137.5, 131.2, 128.3, 126.8, 112.5, 51.9, 51.0, 28.0, 27.1, 16.1; HRESI-MS

m/z (M + H$^+$), Anal. for C$_{19}$H$_{25}$N$_4$O$_2$S: Calc. mass: 373.1698. Found: 373.1688; Anal HPLC

(70:30 H$_2$O/0.1% TFA:CH$_3$CN/0.1% TFA→100% CH$_3$CN/0.1% TFA over 30 min, t_r = 36.1

min).

Methyl 3-amino-5-(azepan-1-yl)-6-(4-(trifluoromethyl)phenyl)pyrazine-2-carboxylate (11a)

General Method A using 4-(trifluoromethyl)phenyl boronic acid (570 mg, 3.0 mmol) afforded

11a as a white solid; yield 64% (505 mg, 1.28 mmol); MP 158-160 °C; ^{1}H NMR (500 MHz,

CDCl$_3$): δ 7.63 (s, 4H), 6.13 (br s, 2H, NH$_2$), 3.89 (s, 3H), 3.34 (s, 4H), 1.65 (s, 4H), 1.45 (s,

4H); ^{13}C NMR (126 MHz, CDCl$_3$): δ 167.4, 154.9, 153.7, 144.6, 129.9, 129.3, 128.2, 125.6,

125.1, 113.2, 52.1, 51.3, 28.1, 27.3; HRESI-MS *m/z* (M + Na$^+$) Anal. For C$_{19}$H$_{21}$F$_3$N$_4$NaO$_2$:

Calc. mass 417.1526. Found 417.1514; Anal-HPLC (100% H$_2$O/0.1% TFA→100%

CH$_3$CN/0.1% TFA over 30 min, t_r = 29.3 min).

Methyl 3-amino-5-(azepan-1-yl)-6-(benzo[d][1,3]dioxol-5-yl)pyrazine-2-carboxylate (12a)

General Method A using benzo[d][1,3]dioxol-5-ylboronic acid (85 mg, 0.515 mmol) afforded

12a as a yellow solid; yield 51% (66 mg, 0.178 mmol). MP: 156-158 °C; ^{1}H NMR (500 MHz,

CDCl$_3$) δ 7.02 (s, 1H), 6.93 (d, *J* = 8.0 Hz, 1H), 6.80 (d, *J* = 8.0 Hz, 1H), 5.96 (s, 2H), 3.88 (s,

4H), 3.38 (s, 4H), 1.63 (s, 4H), 1.44 (s, 4H); ^{13}C NMR (126 MHz, CDCl$_3$) δ 167.6, 154.9, 153.5,

147.9, 147.1, 134.9, 131.5, 121.7, 112.2, 108.7, 108.3, 101.1, 51.9, 51.0, 28.1, 27.1; HRESI-MS m/z (M + H$^+$) Anal. for $C_{19}H_{23}N_4O_4$: Calc. Mass 371.1719. Found 371.1734; Anal HPLC (100 H_2O/0.1% TFA→100% CH_3CN/0.1% TFA over 30 min, t_r = 31.8 min).

Methyl 3-amino-5-(azepan-1-yl)-6-(isoquinolin-4-yl)pyrazine-2-carboxylate (13a)

General Method A using isoquinolin-4-yl boronic acid (271 mg, 1.06 mmol) afforded **13a** as a brown solid; yield 58% (156 mg, 0.413 mmol); MP 140-142 °C; ^{1}H NMR (500 MHz, CDCl$_3$) δ 9.23 (s, 1H), 8.58 (s, 1H), 8.00 (d, J = 8.0 Hz, 1H), 7.81 (d, J = 8.0 Hz, 1H), 7.68 (t, J = 7.5 Hz, 1H), 7.62 (t, J = 7.5 Hz, 1H), 3.86 (s, 3H), 3.21 (t, J = 5.5 Hz, 4H), 1.47 (s, 4H), 1.38 (s, 4H); ^{13}C NMR (126 MHz, CDCl$_3$) δ 167.3, 155.8, 154.0, 152.1, 143.0, 134.3, 131.8, 130.8, 128.4, 128.0, 127.4, 126.7, 124.5, 112.9, 52.0, 50.4, 27.8, 26.8; HRESI-MS m/z (M + Na$^+$) 400, Anal. for $C_{21}H_{24}N_5NaO_2$: Calc. Mass 400.1749. Found 400.1747; Anal HPLC (100% H_2O/0.1% TFA→100% CH_3CN/0.1% TFA over 30 min, t_r = 22.3 min).

Methyl 3-amino-5-(azepan-1-yl)-6-(1-methyl-1H-pyrazol-4-yl)pyrazine-2-carboxylate (14a)

General Method A using 1-methyl-1H-pyrazol-4-yl boronic acid (110 mg, 0.526 mmol) afforded **14a** as a yellow solid; yield 77% (89 mg, 0.269 mmol). MP: 134-136 °C; ^{1}H NMR (500 MHz, CDCl$_3$) δ 7.64 (s, 1H), 7.57 (s, 1H), 6.17 (bs, 2H), 3.91 (s, 3H), 3.89 (s, 3H), 3.47 (t, J = 6 Hz, 4H), 1.66 (s, 4H), 1.47 (s, 4H); ^{13}C NMR (126 MHz, CDCl$_3$) δ 167.4, 155.5, 153.4, 138.7, 129.1, 125.3, 122.6, 112.4, 52.1, 51.2, 39.0, 28.0, 27.2; HRESI-MS m/z (M + H$^+$) 331, Anal. for $C_{16}H_{23}N_6O_2$: Calc. Mass 331.1882. Found 331.1894; Anal HPLC (70:30 H_2O/0.1% TFA: CH_3CN/0.1% TFA→100% CH_3CN/0.1% TFA over 30 min, t_r = 25.2 min).

Methyl 3-amino-5-(azepan-1-yl)-6-(1-(2-morpholinoethyl)-1H-pyrazol-4-yl)pyrazine-2-carboxylate (15a)

General Method A using 1-(2-morpholinoethyl)-1H-pyrazol-4-yl boronic acid (165 mg, 0.536 mmol) afforded **15a** as a yellow solid; yield 80% (119 mg, 0.277 mmol). MP: 132-134 °C; ^{1}H NMR (500 MHz, CDCl$_3$) δ 7.70 (s, 1H), 7.61 (s, 1H), 6.24 (bs, 2H), 4.25 (s, 2H), 3.89 (s, 3H), 3.69 (s, 4H), 3.46 (s, 4H), 2.84 (s, 2H), 2.50 (s, 4H), 1.65 (s, 4H), 1.47 (s, 4H); ^{13}C NMR (126 MHz, CDCl$_3$) δ 167.2, 155.5, 153.3, 138.6, 128.7, 125.2, 122.1 112.4, 66.9, 58.2, 53.7, 51.9, 51.1, 49.6, 27.9 27.0; HRESI-MS *m/z* (M + H$^+$), Anal. for C$_{22}$H$_{36}$N$_7$O$_3$: Calc. mass 430.2567. Found 430.2553; Anal HPLC (70:30 H$_2$O/0.1% TFA: CH$_3$CN/0.1% TFA →100% CH$_3$CN/0.1% TFA over 30 min, t_r = 21.6 min).

Methyl 3-amino-5-(azepan-1-yl)-6-(1H-indol-2-yl)pyrazine-2-carboxylate (16a)

General Method A using 1*H*-indol-2-yl boronic acid (278 mg, 1.73 mmol) afforded **16a** as an orange solid; yield 34% (87.5 mg, 0.239 mmol). MP 152-154 °C; ^{1}H NMR (500 MHz, CDCl$_3$) δ 9.14 (s, 1H), 7.57 (d, 1H), 7.37 (d, 1H, *J* = 7.7 Hz), 7.16 (t, 1H, *J* = 7.0 Hz), 7.08 (t, 1H, *J* = 7.0 Hz), 6.52 (s, 1H), 3.93 (s, 3H), 3.58 (t, *J* = 5.75 Hz, 4H), 1.70 (s,4H), 1.50 (s, 4H); ^{13}C NMR (126 MHz, CDCl$_3$) δ 167.2, 155.1, 153.2, 136.0, 135.7, 129.0, 124.5, 122.4, 120.7, 119.90, 112.70, 111.0, 102.0, 52.1, 51.7, 28.1, 27.5; HRESI-MS *m/z* (M + H$^+$) 388, Anal. for C$_{20}$H$_{24}$N$_5$O$_2$: Calc. mass 388.1730. Found 388.1731; Anal HPLC (100 H$_2$O/0.1% TFA→100% CH$_3$CN/0.1% TFA over 30 min, t_r = 29.8 min).

Methyl 3-amino-5-(azepan-1-yl)-6-(benzo[b]thiophen-2-yl)pyrazine-2-carboxylate (17a)

General Method A using benzo[b]thiophen-2-yl boronic acid (534 mg, 3.0 mmol) afforded **17a** as a yellow solid; yield 78% (600 mg); MP 146-148 °C; ^{1}H NMR (500 MHz, CDCl$_3$): δ 1.48 (s, 4H), 1.69 (s, 4H), 3.51 (s, 4H), 3.91 (s, 3H), 6.13 (br s, 2H, NH2), 7.22 (s, 1H), 7.21 (m, 2H), 7.71 (d, J = 6.9 Hz, 1H), 7.80 (d, J = 7.0 Hz, 1H); ^{13}C NMR (126 MHz, CDCl$_3$): δ 167.3, 155.3, 153.6, 143.3, 140.2, 140.1, 125.4, 124.5, 124.4, 123.6, 122.3, 122.0, 113.2, 52.3, 51.3, 28.2, 27.4; HRESI-MS m/z (M + K$^+$) Anal for C$_{20}$H$_{22}$KN$_4$O$_3$ Calc. mass 405.1394. Found 405.1361; Anal-HPLC (100 H$_2$O/0.1% TFA→100% CH$_3$CN/0.1% TFA over 30 min, t_r = 31.9 min).

Methyl 3-amino-5-(azepan-1-yl)-6-(benzofuran-2-yl)pyrazine-2-carboxylate (18a)

General Method A using benzofuran-2-yl boronic acid (486 mg, 3.0 mmol) afforded **18a** as a yellow solid; yield 57% (420 mg). MP: 121-123 °C; ^{1}H NMR (500 MHz, CDCl$_3$): δ 1.46 (s, 4H), 1.66 (s, 4H), 3.45 (t, J = 5.8 Hz, 4H), 3.90 (s, 3H), 6.13 (br s, 2H, NH2), 6.93 (s, 1H), 7.21 (t, J = 7.3 Hz, 1H), 7.25 (t, J = 7.2 Hz, 1H), 7.47 (d, J = 7.9 Hz, 1H), 7.56 (d, J = 7.5 Hz, 1H); ^{13}C NMR (126 MHz, CDCl$_3$): δ 167.2, 164.9, 154.8, 154.6, 129.2, 124.4, 123.1, 121.4, 121.2, 112.9, 111.5, 105.1, 52.2, 50.2, 28.2, 27.3; HRESI-MS m/z (M + H$^+$) Anal for C$_{20}$H$_{23}$N$_4$O$_2$: Calc. mass 367.1831. Found. 367.1770; Anal-HPLC (70:30 H$_2$O/0.1%: CH$_3$CN/0.1% TFA→100% CH$_3$CN/0.1% TFA over 30 min, t_r = 29.5 min).

Methyl 3-amino-5-(azepan-1-yl)-6-(4-fluorobenzofuran-2-yl)pyrazine-2-carboxylate (19a)

General Method A using 4-fluorobenzofuran-2-yl boronic acid (95 mg, 0.531 mmol) afforded **19a** as a yellow solid; yield 58% (80 mg, 0.210 mmol). MP: 108-110 °C; ^{1}H NMR (126 MHz, CDCl$_3$): 7.27 (d, 1H), 7.20 (m, 1H), 6.99 (s, 1H), 6.93 (t, 1H, J = 8.5 Hz), 3.91 (s, 3H), 3.46 (s, 4H), 1.69 (s, 4H), 1.49 (s, 4H); ^{13}C NMR (126 MHz, CDCl$_3$) δ 167.0, 156.9, 156.2, 154.7, 154.0,

138.3, 124.6, 120.5, 118.0, 115.9, 110.4, 108.6, 107.6, 52.2, 50.0, 28.0, 27.1; HRESI-MS m/z (M + Na$^+$) Anal. for C$_{20}$H$_{21}$FN$_6$NaO$_4$: Calc. mass 407.1495. Found 407.1504; Anal HPLC (70:30 H$_2$O/0.1% TFA: CH$_3$CN/0.1% TFA$\rightarrow$100% CH$_3$CN/0.1% TFA over 30 min, t_r = 21.2 min).

Methyl-3-amino-5-(azepan-1-yl)-N-carbamimidoyl-6-(thiophen-2-yl)pyrazine-2-carboxamide (20a)

General Method A using thiophen-2-yl boronic acid (70 mg, 0.549 mmol) afforded **20a** as a light yellow solid; yield 85% (99 mg, 0.299 mmol). MP: 118-120 °C; ^{1}H NMR (500 MHz, CDCl$_3$) δ 7.27 (d, J = 5 Hz, 1H), 7.03 (d, J = 3 Hz, 1H), 6.98 (m, 1H), 3.89 (s, 3H), 3.43 (t, J = 5.7 Hz, 4H), 1.67 (s, 4H), 1.47 (s, 4H); ^{13}C NMR (126 MHz, CDCl$_3$) δ 167.3, 155.2, 153.5, 142.8, 126.9, 126.0, 125.8, 125.5, 112.7, 52.1, 51.1, 28.2, 27.3; HRESI-MS m/z (M + Na$^+$) Anal. for C$_{16}$H$_{20}$N$_4$NaO$_2$: Calc. mass 355.1205. Found 355.1193; Anal HPLC (100 H$_2$O/0.1% TFA $\rightarrow$100% CH$_3$CN/0.1% TFA over 30 min, t_r = 28.8 min).

Methyl 3-amino-5-(azepan-1-yl)-6-(thiophen-3-yl)pyrazine-2-carboxylate (21a)

General Method A using thiophen-3-yl boronic acid (75 mg, 0.584 mmol) afforded **21a** as a white solid; yield 85% (100 mg, 0.302 mmol). MP: 118-120°C; ^{1}H NMR (500 MHz, CDCl$_3$) δ 7.38 (s, 1H), 7.29 (m, 1H), 7.25 (d, J = 5 Hz, 1H), 3.88 (s, 3H), 3.38 (t, J = 5.8 Hz, 4H), 1.63 (s, 4H), 1.44 (s, 4H); ^{13}C NMR (126 MHz, CDCl$_3$) δ 167.4, 155.3, 153.5, 141.3, 128.1, 127.9, 125.4, 122.8, 112.2, 52.0, 50.9, 28.0, 27.1; HRESI-MS m/z (M + H$^+$) Anal. for C$_{16}$H$_{21}$N$_4$NaO$_2$S: Calc. mass 355.1205. Found 355.1197; Anal HPLC (100 H$_2$O/0.1% TFA$\rightarrow$100% CH$_3$CN/0.1% TFA over 30 min, t_r = 28.3 min).

Methyl 3-amino-5-(azepan-1-yl)-6-(furan-2-yl)pyrazine-2-carboxylate (22a)

General Method A using furan-2-ylboronic acid (59 mg, 0.526 mmol) afforded **22a** as an off white solid; yield 98% (111 mg, 0.352 mmol). MP 116-118 °C; ^{1}H NMR (500 MHz, CDCl$_3$): δ 7.41 (s, 1H), 6.54 (d, J = 2.3 Hz, 1H), 6.45 (s, 1H), 6.13 (br s, 2H, NH$_2$), 3.89 (s, 3H), 3.37 (t, J = 5.5 Hz, 4H), 1.66 (s, 4H), 1.47 (s, 4H); ^{13}C NMR (126 MHz, CDCl$_3$): δ 167.1, 154.8, 154.0, 152.2, 141.4, 122.0, 112.1, 111.6, 108.6, 52.0, 50.0, 28.0, 26.9; HRESI-MS m/z (M + Na$^+$) Anal. for C$_{16}$H$_{21}$N$_4$NaO$_3$: Calc. mass 339.1418. Found 339.1433; Anal-HPLC (100 H$_2$O/0.1% TFA→100% CH$_3$CN/0.1% TFA over 30 min, t_r = 27.1 min).

Methyl 3-amino-5-(azepan-1-yl)-6-(furan-3-yl)pyrazine-2-carboxylate (23a)

General Method A using furan-3-yl boronic acid (107 mg, 0.389 mmol) afforded **23a** as a yellow solid; yield 93% (114 mg, 0.360 mmol). MP: 122-124° C; ^{1}H NMR (500 MHz, CDCl$_3$) δ 7.64 (s, 1H), 7.41 (s, 1H), 6.61 (s, 1H), 6.20 (bs, 2H), 3.89 (s, 3H), 3.48 (t, J = 5 Hz, 4H), 1.66 (s, 4H), 1.47 (s, 4H); ^{13}C NMR (126 MHz, CDCl$_3$) δ 167.3, 155.6, 153.6, 142.6, 140.6, 125.8, 124.8, 112.6, 111.2, 52.0, 51.0, 28.0, 27.1; HRESI-MS m/z (M + H$^+$) Anal. for C$_{16}$H$_{21}$N$_4$O$_3$: Calc. mass 316.1614. Found 316.1604; Anal HPLC (70:30 H$_2$O/0.1% TFA: CH$_3$CN/0.1% TFA→100% CH$_3$CN/0.1% TFA over 30 min, t_r = 30.9 min).

Methyl 3-amino-5-(azepan-1-yl)-6-(2-fluoropyridin-3-yl)pyrazine-2-carboxylate (24a)

General Method A using 2-fluoropyridin-3-yl boronic acid (75 mg, 0.529 mmol) afforded **24a** as a brown solid; yield 76% (92 mg, 0.266 mmol). MP: 156-158°C; ^{1}H NMR (500 MHz, CDCl$_3$) δ 8.17 (d, J = 4.3 Hz, 1H), 8.06 (m, 1H), 7.29 (t, J = 5.5 Hz, 1H), 3.89 (s, 3H), 3.36 (s, J = 5.7 Hz, 4H), 1.63 (s, 4H), 1.46 (s, 4H); ^{13}C NMR (126 MHz, CDCl$_3$) δ 167.2, 161.3, 155.2, 154.1,

146.8, 141.1, 124.5, 123.8, 122.2, 113.3, 52.3, 50.3, 28.1, 27.3; HRESI-MS m/z (M + Na$^+$) Anal. for $C_{17}H_{20}FN_5NaO_2$: Calc. mass 368.1499. Found 368.1489; Anal HPLC (100 H$_2$O/0.1% TFA→100% CH$_3$CN/0.1% TFA over 30 min, t_r = 26.3 min).

Methyl 3-amino-5-(azepan-1-yl)-6-(pyrimidin-5-yl)pyrazine-2-carboxylate (25a)

General Method A using pyrimidin-5-yl boronic acid (279 mg, 2.25 mmol) afforded **25a** as a yellow solid; yield 91% (450 mg). MP 176-178 °C; ^{1}H NMR (500 MHz, CDCl$_3$): δ 9.13 (s, 1H), 8.89 (s, 2H), 6.13 (br s, 2H, NH2), 3.91 (s, 3H), 3.52 (t, J = 6.0 Hz, 4H), 1.68 (s, 4H), 1.48 (s, 4H); ^{13}C NMR (126 MHz, CDCl$_3$): δ 167.1, 157.1, 155.7, 155.3, 153.9, 134.9, 124.5, 114.5, 52.3, 51.5, 28.0, 27.4; HRESI-MS m/z (M + Na$^+$) Anal. for $C_{16}H_{20}N_6NaO_2$: Calc mass 351.1545. Found. 351.1535; Anal-HPLC (70:30 H$_2$O/0.1% TFA: CH$_3$CN/0.1% TFA→100% CH$_3$CN/0.1% TFA over 30 min, t_r = 23.4 min).

Methyl 3-amino-5-(azepan-1-yl)-6-(2-methoxypyrimidin-5-yl)pyrazine-2-carboxylate (26a)

General Method A using 2-methoxypyrimidin-5-yl boronic acid (79 mg, 0.513 mmol) afforded **26a** as a yellow solid; yield 88% (111 mg, 0.310 mmol). MP 168-170 °C; ^{1}H NMR (500 MHz, CDCl$_3$): 8.66 (s, 2H), 6.13 (br s, 2H, NH$_2$), 4.05 (s, 3H), 3.90 (s, 3H), 3.38 (t, J = 5.5 Hz, 4H), 1.68 (s, 4H), δ 1.48 (s, 4H); ^{13}C NMR (126 MHz, CDCl$_3$): δ 166.4, 164.7, 158.3, 155.3, 153.8, 128.8, 125.2, 113.9, 55.2, 52.2, 51.4, 28.0, 27.3; HRESI-MS m/z (M + H$^+$) Anal. for $C_{17}H_{22}N_6O_3$: Calc. mass 359.1832. Found 359.1848; Anal-HPLC (70:30 H$_2$O/0.1% TFA: CH$_3$CN/0.1% TFA→100% CH$_3$CN/0.1% TFA over 30 min, t_r = 28.0 min).

Methyl 3-amino-5-(azepan-1-yl)-6-(2,4-dimethoxypyrimidin-5-yl)pyrazine-2-carboxylate (27a)

General Method A using 2,4-dimethoxypyrimidin-5-yl boronic acid (79 mg, 0.350 mmol) afforded **27a** as a yellow solid; yield 91% (124 mg, 0.319 mmol). MP 150-152 °C; ^{1}H NMR (500 MHz, CDCl$_3$) δ 8.36 (s, 1H), 4.03 (s, 3H), 3.94 (s, 3H), 3.87 (s, 3H), 3.39 (s, 4H), 1.60 (s, 4H,), 1.46 (s, 4H); ^{13}C NMR (126 MHz, CDCl$_3$) δ 168.3, 167.2, 164.8, 158.1, 155.3, 154.1, 123.8, 117.1, 112.6, 55.0, 54.1, 52.0, 50.0, 28.0, 27.0; HRESI-MS m/z (M + H$^+$) Anal. for C$_{18}$H$_{25}$N$_6$O$_4$ Calc. mass 389.1937. Found389.1929; Anal-HPLC (70:30 H$_2$O/0.1% TFA: CH$_3$CN/0.1% TFA→100% CH$_3$CN/0.1% TFA over 30 min, t_r = 27.1 min).

Methyl 3-amino-5-(azepan-1-yl)-6-(2,6-dimethoxypyridin-3-yl)pyrazine-2-carboxylate (28a)

General Method A using 2,6-dimethoxypyridin-3-yl boronic acid (200 mg, 0.703 mmol) afforded **28a** as a yellow solid; yield 42% (115 mg, 0.297 mmol); MP: 134-136 °C; ^{1}H NMR (500 MHz, CDCl$_3$) δ 7.66 (d, J = 8.0 Hz, 1H), 6.38 (d, J = 8.0 Hz, 1H), 3.92 (s, 3H), 3.87 (s, 3H), 3.86 (s, 3H), 3.45 (bs, 2H), 3.31 (bs, 2H), 1.57 (s, 4H), 1.44 (s, 4H); ^{13}C NMR (126 MHz, CDCl$_3$) δ 167.5, 162.8, 159.7, 155.3, 153.9, 141.5, 127.6, 116.2, 112.2, 101.3, 53.7, 53.5, 51.9, 50.1, 28.1, 27.1; HRESI-MS m/z (M + H$^+$), Anal. for C$_{19}$H$_{25}$N$_5$O$_4$: Calc. mass 388.1985. Found 388.1983; Anal HPLC (70:30 H$_2$O/0.1% TFA: CH$_3$CN/0.1% TFA→100% CH$_3$CN/0.1% TFA over 30 min, t_r = 31.6 min).

Methyl 3-amino-5-(azepan-1-yl)-6-(2,4-dimethoxyphenyl)pyrazine-2-carboxylate (29a)

General Method A using 2,4-dimethoxyphenyl boronic acid (128 mg, 0.702 mmol) afforded **29a** as a yellow solid; yield 53% (143 mg, 0.371 mmol). MP: 106-108 °C; ^{1}H NMR (500 MHz,

CDCl$_3$): δ 7.33 (d, *J* = 8.3 Hz, 1H), 6.54 (dd, *J* = 8.3 Hz, *J* = 2.1 Hz 1H), 6.42 (d, *J* = 2.1 Hz, 1H), 3.85 (s, 3H), 3.82 (s, 3H), 3.70 (s, 3H), 3.44 (s, 2H), 3.26 (s, 2H), 1.58 (s, 2H), 1.53 (s, 2H), 1.46 (s, 2H), 1.39 (s, 2H); ^{13}C NMR (126 MHz, CDCl$_3$) δ 166.0, 160.9, 158.2, 155.4, 154.0, 131.1, 129.2, 123.7, 111.8, 105.1, 98.7, 55.7, 55.7, 52.0, 50.6, 27.8, 26.9; HRESI-MS *m/z* (M + Na$^+$), Anal. for C$_{20}$H$_{27}$N$_4$NaO$_4$: Calc. mass 409.1852. Found 409.1866; Anal HPLC (100 H$_2$O/0.1% TFA→100% CH$_3$CN/0.1% TFA over 30 min, t_r = 28.6 min).

Methyl 3-amino-5-(azepan-1-yl)-6-(3,5-dimethoxyphenyl)pyrazine-2-carboxylate (30a)

General Method A using 3,5-dimethoxyphenyl boronic acid (128 mg, 0.702 mmol) afforded **30a** as a yellow solid; 62% (166 mg, 0.430 mmol). MP: 96-98 ° C; ^{1}H NMR (500 MHz, CDCl$_3$) δ 6.64 (s, 2H), 6.40 (s, 1H), 3.88 (s, 3H), 3.81 (s, 6H), 3.38 (t, *J* = 6.0 Hz, 4H), 1.64 (s, 4H), 1.44 (s, 4H); ^{13}C NMR (126 MHz, CDCl$_3$) δ 167.5, 161.0, 154.7, 153.7, 142.8, 131.6, 112.0, 106.3, 100.0, 55.6, 52.0, 50.9, 28.1, 27.1; HRESI-MS *m/z* (M + Na$^+$), Anal. for C$_{20}$H$_{26}$N$_4$NaO$_4$: Calc. mass 409.1852. Found 409.1867; Anal HPLC (70:30 H$_2$O/0.1% TFA: CH$_3$CN/0.1% TFA→100% CH$_3$CN/0.1% TFA over 30 min, t_r = 30.0 min).

Methyl 3-amino-5-(azepan-1-yl)-6-(3,6-dimethoxypyridazin-4-yl)pyrazine-2-carboxylate (31a)

General Method A using 3,6-dimethoxypyridazin-4-yl boronic acid (97 mg, 0.526 mmol) afforded **31a** as a yellow solid; yield 68% (94 mg, 0.242 mmol): MP: 152-154 °C; ^{1}H NMR (500 MHz, CDCl$_3$) δ 7.17 (s, 1H), 4.08 (s, 3H), 4.00 (s, 3H), 3.88 (s, 3H), 3.43 (s, 2H), 3.29 (s, 2H), 1.63 (s, 4H), 1.44 (s, 4H); ^{13}C NMR (126 MHz, CDCl$_3$) δ 167.00, 162.8, 159.6, 154.7, 154.1, 135.1, 122.9, 119.4, 113.1, 54.8, 54.6, 52.1, 49.7, 28.0, 27.2; HRESI-MS *m/z* (M + Na$^+$), Anal.

for $C_{18}H_{24}N_6NaO_4$: Calc. mass 411.1757. Found 411.1762; Anal HPLC (70:30 H_2O/0.1% TFA: CH_3CN/0.1% TFA→100% CH_3CN/0.1% TFA over 30 min, t_r = 21.2 min).

Methyl 3-amino-6-(2-aminopyrimidin-5-yl)-5-(azepan-1-yl)pyrazine-2-carboxylate (32a)

General Method A using 2-aminopyrimidin-5-yl boronic acid (208 mg, 1.5 mmol) afforded **32a** as a yellow solid; yield 83% (285 mg). MP: 216-218 °C; ^{1}H NMR (500 MHz, DMSO-d_6): δ 8.27 (s, 2H), 7.04 (br s, 2H, NH$_2$), 6.76 (br s, 2H, NH$_2$), 3.74 (s, 3H), 3.41 (t, J = 5.9 Hz, 4H), 1.59 (s, 4H), 1.41 (s, 4H); ^{13}C NMR (126 MHz, DMSO-d_6): δ 27.0, 27.9, 51.0, 51.9, 112.3, 123.9, 126.5, 154.2, 155.1, 157.4, 163.0, 167.3, 163.0, 157.4, 155.1, 154.2, 126.5, 123.9, 112.3, 51.9, 51.0, 27.9, 27.0; HRESI-MS m/z (M + H$^+$), Anal. for $C_{16}H_{22}N_7O_2$: Calc. mass 344.1835. Found 344.1833; Anal HPLC (100 H_2O/0.1% TFA→100% CH_3CN/0.1% TFA over 30 min, t_r = 14.2 min).

Methyl 3-amino-5-(azepan-1-yl)-6-(2-chloropyrimidin-5-yl)pyrazine-2-carboxylate (8)

General Method A using (2-chloropyrimidin-5-yl)boronic acid (475 mg, 3 mmol) afforded **8** as a yellow solid; (460 mg, 64%); MP 168-170 °C; ^{1}H NMR (CDCl$_3$): δ 8.76 (s, 2H), 6.13 (br s, 2H, NH$_2$), 3.91 (s, 3H), 3.35 (t, J = 5.8 Hz, 4H), 1.71 (s, 4H), 1.49 (s, 4H); ^{13}C NMR (CDCl$_3$): δ 27.3, 27.8, 51.4, 52.2, 114.6, 122.8, 133.3, 153.7, 155.0, 158.0, 159.2, 166.8; MS (ESI): m/z 363 (M+H)$^+$, 385 (M+H)$^+$; HRESI-MS m/z (M + H$^+$), Anal. for $C_{16}H_{20}ClN_6O_2$: Calc. mass 363.1336. Found 363.1347; Anal HPLC (100 H_2O/0.1% TFA→100% CH_3CN/0.1% TFA over 30 min, t_r = 17.6 min).

General Method B: Synthesis of methyl 3-amino-5-(azepan-1-yl)-6-(2-(substituted amino)pyrimidin-5-yl)pyrazine-2-carboxylates 33a and 34a

To a solution of methyl 3-amino-5-(azepan-1-yl)-6-(2-chloropyrimidin-5-yl)pyrazine-2-carboxylate **8** (0.25 mmol) in DMF (2 mL) at room temperature was added the appropriate amine (0.75 mmol). Diisopropylethylamine (0.75 mmol) was then added and the reaction mixture was stirred at room temperature for 2 days. The mixture was extracted with EtOAc (3 x 10 mL) and the combined organic layer was washed with brine, dried (MgSO$_4$) and evaporated. The residue was purified by silica gel flash column chromatography using EtOAc/pet spirit.

Methyl 3-amino-5-(azepan-1-yl)-6-(2-(methylamino)pyrimidin-5-yl)pyrazine-2-carboxylate (33a)

General Method B using **8** (91 mg, 0.25 mmol) and methylamine (2M in MeOH, 0.375 mL, 0.75 mmol) gave **33a** as a yellow solid; yield 87% (78.0 mg). MP: 158-160 °C. ^{1}H NMR (500 MHz, CDCl$_3$): δ 8.45 (s, 2H), 6.22 (br s, 2H, NH$_2$), 5.28 (q, J = 4.9 Hz, 1H, NH), 3.90 (s, 3H), 3.42 (t, J = 5.9 Hz, 4H), 3.04 (d, J = 5.1 Hz, 3H), 1.67 (s, 4H), δ 1.47 (s, 4H); ^{13}C NMR (126 MHz, CDCl$_3$): δ 167.4, 162.0, 157.2, 155.3, 153.7, 126.9, 124.2, 113.3, 52.3, 51.3, 28.8, 28.0, 27.3; HRESI-MS m/z (M + H$^+$), Anal. for C$_{17}$H$_{24}$N$_7$O$_2$ 358.1991, found 358.2001; Anal HPLC (100 H$_2$O/0.1% TFA→100% CH$_3$CN/0.1% TFA over 30 min, t_r = 14.8 min)

Methyl 3-amino-5-(azepan-1-yl)-6-(2-(isopropylamino)pyrimidin-5-yl)pyrazine-2-carboxylate (34a)

General Method B using **8** (91 mg, 0.25 mmol) and isopropylamine (45 mg, 0.75 mmol) gave **34a** as a yellow solid; yield 83% (80 mg). MP: 155-157 °C. ^{1}H NMR (500 MHz, CDCl$_3$): δ 8.43

(s, 2H), 6.25 (br s, 2H), 5.10 (d, J = 7.8 Hz, 1H), 4.16 (septet, J = 6.8 Hz, 1H), 3.89 (s, 3H), 3.43 (t, J = 5.9 Hz, 4H), 1.67 (s, 4H), 1.47 (s, 4H), 1.25 (d, J = 7.0 Hz, 6H); ^{13}C NMR (126 MHz, CDCl$_3$): δ 167.2, 157.0, 155.1, 153.5, 126.8, 123.8, 113.1, 52.0, 51.1, 43.0, 27.8, 27.1, 22.9; HRESI-MS m/z (M + H$^+$), Anal. for for C$_{19}$H$_{28}$N$_7$O$_2$ 386.2304, found 386.2318; Anal HPLC (100 H$_2$O/0.1% TFA→100% CH$_3$CN/0.1% TFA over 30 min, t_r = 16.1 min)

Methyl 3-amino-5-(azepan-1-yl)-6-(2-(2-hydroxyethyl)amino)pyrimidin-5-yl)pyrazine-2-carboxylate (35a)

To a solution of methyl 3-amino-5-(azepan-1-yl)-6-(2-chloropyrimidin-5-yl)pyrazine-2-carboxylate **8** (91 mg, 0.25 mmol) in 2-propanol (5 mL) was added ethanolamine (16.8 mg, 0.017 mL, 0.275 mmol). Diisopropyethylamine (35.5 mg, 0.048 mL, 0.275 mmol) was then added and the reaction mixture was heated at reflux for 2 hours. After cooling to room temperature, additional equivalents of ethanolamine (0.275 mmol) and DIPEA (0.275 mmol) were added and the reaction mixture was heated for a further 2 h. The mixture was allowed to cool to room temperature overnight, which caused the product to crystallize. The solid product was collected by vacuum filtration and washed with cold 2-propanol (2 x 2 mL) and diethyl ether (2 mL). After drying, the pure product was obtained as light yellow crystals (82 mg, 84%). MP: 164-166 °C ^{1}H NMR (500 MHz, CDCl$_3$): δ, 8.44 (s, 2H), 6.23 (br s, 2H), 5.64 (t, J = 5.5 Hz, 1H), 3.90 (s, 3H), 3.85 (t, J = 4.4 Hz, 2H), 3.62 (q, J = 4.9 Hz, 2H), 3.42 (t, J = 5.6 Hz, 4H), 1.68 (s, 4H), 1.48 (s, 4H); ^{13}C NMR (126 MHz, CDCl$_3$): δ 167.1, 161.7, 156.9, 155.1, 153.5, 126.2, 124.6, 113.3, 63.6, 52.1, 51.1, 44.9, 27.8, 27.1; HRESI-MS m/z (M + H$^+$), Anal. for C$_{18}$H$_{26}$N$_7$O$_3$ 388.2097, found 388.2088; Anal HPLC (100 H$_2$O/0.1% TFA→100% CH$_3$CN/0.1% TFA over 30 min, t_r = 14.4 min).

General Method C: Synthesis of acyl guanidines using the reported method[40]

Free guanidine was generated via neutralization of guanidine.HCl with Na$^+$ iPrO$^-$ in iPrOH to create a 2-fold molar excess relative to the 6-substituted pyrazinoyl methyl ester. A stock solution of iPrO$^-$ was prepared by adding Na (typically 30-70 mg) in anhydrous iPrOH under N$_2$ and heated at 70 °C for 30 min. From this stock solution an amount of iPrO$^-$ was removed via syringe and made up to 10 mL in anhydrous iPrOH. To this solution was added a stoichiometric amount of guanidine hydrochloride and the mixture stirred at 70 °C for 30 min. This solution was gravity filtered onto the neat 6-substituted pyrazinoyl methyl ester. Once filtration was complete, the mixture was heated to reflux and allowed to react for 1-6 h. The reactions were monitored by MS and TLC and terminated by removal of solvent under reduced pressure. Final products were isolated by rp-HPLC. All compounds were isolated as TFA salts and exchanged to their respective HCl salts by stirring with quaternary ammonium Cl$^-$ anion exchange resin in MeOH prior to biological evaluation.

General Method D: Improved Synthesis of Acyl Guanidines

Dry CH$_3$OH (50 mL) was slowly added with stirring to small pieces of sodium (2.3 g, 0.1 mol) cooled on ice under nitrogen. After complete dissolution of the sodium, guanidine hydrochloride (9.55 g, 0.1 mol) was added and the resulting mixture was stirred at room temperature for 1.5 h. Filtration of the white precipitate gave a 2 M solution of free guanidine in methanol, which was collected in a sealed dry flask under nitrogen and stored in a refrigerator.

To a suspension of the requisite methyl ester (1 eq, 0.2-0.5 mmol) in DMF (5 mL) was added 2 M guanidine in methanol (10 eq, 2-5 mmol) and the resulting mixture was stirred at room temperature overnight. Brine (20 mL) was added and the mixture extracted with EtOAc (3 x 30 mL). The organic layer was washed with 10% NaCl (2 x 30 mL), dried (MgSO$_4$), and concentrated under reduced pressure. The crude mixture was dissolved in 5 mL of 30% CH$_3$CN:

70% H_2O and 0.1 % acetic acid and loaded onto a reverse phase silica gel chromatography column. Isocratic elution was performed with $CH_3CN:H_2O$ mixtures containing 0.1 % acetic acid). The pooled fractions containing pure compound by TLC analysis were concentrated under reduced pressure and neutralised with solid $NaHCO_3$. The aqueous mixture was extracted with EtOAc (3 x 30 mL) and the combined organic layer was washed with brine, dried ($MgSO_4$) and evaporated to give the free acylguanidine.

3-Amino-5-(azepan-1-yl)-N-carbamimidoyl-6-(4-(methylthio)phenyl) pyrazine-2-carboxamide (10)

General Method C using **10a** (70 mg, 0.214 mmol) gave **10** as a yellow solid; yield 5% (6 mg, 0.015 mmol). MP: 152-154 °C; ^{1}H NMR (500 MHz, $CDCl_3$) δ 10.31 (s, 1H), 9.44 (s, 2H), 8.47 (s, 2H), 7.44 (d, J = 8.1 Hz, 2H), 7.28 (d, J = 8.1 Hz, 2H), 3.40 (t, J = 5.5 Hz, 4H) 1.60 (s, 4H), 1.46 (s, 4H); ^{13}C NMR (126 MHz, $CDCl_3$) δ 166.0, 156.6, 155.7, 153.6, 139.0, 136.4, 131.2, 128.1, 126.6, 111.0, 51.5, 27.9, 27.1, 15.5; HRESI-MS m/z (M + H^{+}) Anal for $C_{19}H_{26}N_7OS$: Calc. mass 400.1920. Found 400.1935; Anal. HPLC. (70:30 H_2O/0.1% TFA: CH_3CN/0.1% TFA→100% CH_3CN/0.1% TFA over 30 min, t_r = 28.4 min).

3-Amino-5-(azepan-1-yl)-N-carbamimidoyl-6-(4-(trifluoromethyl)phenyl) pyrazine-2-carboxamide (11)

General Method D using **11a** (394 mg, 1.0 mmol) gave **11** as a yellow solid; yield 92% (385 mg). MP 172-175 °C; ^{1}H NMR (CD_3OD): δ 7.68 (d, J = 8.0 Hz, 2H), 7.65 (d, J = 8.0 Hz, 2H), 3.38 (t, J = 5.0 Hz, 4H), 1.65 (s, 4H), 1.46 (s, 4H); ^{13}C NMR (CD_3OD): δ 167.9, 160.2, 155.8, 155.0, 145.6, 130.1, 130.0 (d, J = 32 Hz), 129.2, 125.8 (d, J = 2.7 Hz), 124.3 (d, J = 170), 112.9,

51.6, 28.6, 27.6; HRESI-MS m/z (M + H$^+$) Anal for $C_{19}H_{23}F_3N_7O$: Calc. mass 422.1916. Found 422.1911; Anal. HPLC (100% H$_2$O/0.1% TFA→100% CH$_3$CN/0.1% TFA over 30 min, t_r 27.9 min).

3-Amino-5-(azepan-1-yl)-6-(benzo[d][1,3]dioxol-5-yl)-N-carbamimidoyl pyrazine-2-carboxamide (12)

General Method C using **12a** (54 mg, 0.146 mmol) gave **12** as a yellow oil; yield 9% (6 mg, 0.015 mmol). MP: 154-156 °C; ^{1}H NMR (500 MHz, DMSO-d_6) δ 10.39 (s, 1H), 8.71 (s, 2H), 8.27 (s, 2H), 7.31 (s, 1H), 6.96 (m, 2H), 6.08 (s, 2H), 3.40 (t, J= 5.75 Hz, 4H), 1.60 (s, 2H), 1.39 (s, 2H); ^{13}C NMR (126 MHz, DMSO-d_6) δ 166.2, 155.2, 154.8, 153.6, 147.26, 146.7, 133.4, 130.3, 121.4, 112.7, 108.5, 108.0, 101.2, 50.4, 27.2, 26.1; HRESI-MS m/z (M + H$^+$) Anal for $C_{19}H_{24}N_7O_3$: Calc. mass 398.1941. Found 398.1929; Anal. HPLC (70:30 H$_2$O/0.1% TFA: CH$_3$CN/0.1% TFA→100% CH$_3$CN/0.1% TFA over 30 min, t_r 26.4 min).

3-Amino-5-(azepan-1-yl)-N-carbamimidoyl-6-(isoquinolin-4-yl)pyrazine-2-carboxamide (13)

General Method C using **13a** (156 mg, 0.413 mmol) gave **13** as an orange solid; yield 15% (32 mg, 0.079 mmol). MP 158-160 °C; ^{1}H NMR (500 MHz, CD$_3$OD) δ 10.47 (s, exchange with solvent), 9.57 (bs, 1H), 9.19 (s, exchange with solvent), 9.09 (s, exchange with solvent) 8.69 (bs, 1H), 8.40 (d, J = 8.2 Hz, 1H), 8.01 (t, J = 7.5 Hz, 1H), 7.91 (t, J = 7.5 Hz, 1H), 7.81 (d, J = 8.2 Hz, 1H), 3.37 (s, 2H), 3.23 (s, 2H), 1.53 (s, 4H), 1.44 (s, 4H); ^{13}C NMR (126 MHz, CD$_3$OD) δ 167.5, 157.7, 156.9, 156.4, 149.7, 137.6, 136.9, 136.9, 136.8, 131.6, 131.4, 129.0, 125.7, 124.7, 113.0, 51.6, 29.0, 27.8; HRESI-MS m/z (M + H$^+$) Anal for $C_{20}H_{24}N_7OS$: Calc. mass 410.1763.

Found 410.1758; Anal. HPLC (70:30 H_2O/0.1% TFA: CH_3CN/0.1% TFA→100% CH_3CN/0.1%

TFA over 30 min, t_r 22.7 min).

3-Amino-5-(azepan-1-yl)-N-carbamimidoyl-6-(1-methyl-1H-pyrazol-4-yl)pyrazine-2-

carboxamide (14)

General Method C using **14a** (69 mg, 0.207 mmol) gave **14** as a yellow oil; yield 38% (32 mg,

0.193 mmol). MP 150-152 °C; ^1H NMR (500 MHz, CDCl$_3$) δ 10.49 (s, 1H), 8.83 (s, 2H), 8.52

(s, 2H), 8.00 (s, 1H), 7.57 (s, 1H), 5.49 (bs, 2H), 3.93 (s, 3H), 3.50 (t, J = 5.75 Hz, 4H), 1.69 (s,

4H), 1.49 (s, 4H);^{13}C NMR (126 MHz, CDCl$_3$) δ 166.6, 156.4, 156.1, 153.4, 137.4, 130.7, 125.1,

121.7, 111.1, 51.5, 38.7, 27.9, 27.3; HRESI-MS m/z (M + H$^+$) Anal for $C_{16}H_{24}N_9O$: Calc. mass

358.2104. Found 358.2118; Anal HPLC (70:30 H_2O/0.1% TFA: CH_3CN/0.1% TFA→100%

CH_3CN/0.1% TFA over 30 min, t_r = 21.0 min).

3-Amino-5-(azepan-1-yl)-N-carbamimidoyl-6-(1-(2-morpholinoethyl)-1H-pyrazol-4-

yl)pyrazine-2-carboxamide (15)

General Method C using **15a** (99 mg, 0.229 mmol) gave **15** as an orange oil; yield 20% (22

mg, 0.048 mmol). MP: 157-159 °C; ^1H NMR (500 MHz, CDCl$_3$) δ 10.48 (s, 1H), 8.86 (s, 2H),

8.65 (s, 2H), 7.89 (s, 1H), 7.56 (s, 1H), 4.67 (s, 2H), 3.93 (s, 4H), 3.69 (s, 2H,), 3.47 (s, 4H), 3.42

(bs, 2H), 3.05 (bs, 2H,) 1.67 (s, 4H), 1.49 (s, 4H); ^{13}C NMR (126 MHz, CDCl$_3$) δ 166.6, 156.4,

156.1, 153.6, 140.0, 130.6, 124.1, 122.9, 111.3, 63.8, 57.2, 53.3, 51.4, 46.4, 27.9, 27.2; HRESI-

MS m/z (M + H$^+$) Anal for $C_{21}H_{33}N_{10}O_2$: Calc. mass 457.2788. Found 457.2796; Anal. HPLC

(70:30 H_2O/0.1% TFA: CH_3CN/0.1% TFA→100% CH_3CN/0.1% TFA over 30 min, t_r 19.0 min).

3-Amino-5-(azepan-1-yl)-N-carbamimidoyl-6-(1H-indol-2-yl)pyrazine-2-carboxamide (16)

General Method C using **16a** (76 mg, 0.209 mmol) gave **16** as an orange solid; yield 31% (29 mg, 0.074 mmol). MP 152-154 °C; ^{1}H NMR (500 MHz, CDCl$_3$) δ 11.09 (s, 1H), 10.82 (s, 1H), 8.82 (s, 2H), 7.92 (s, 2H), 7.55 (d, 1H, J = 7.7 Hz), 7.41 (d, 1H, J = 7.7 Hz), 7.12 (t, 1H, J = 7 Hz), 7.03 (t, 1H), 6.44 (s, 1H), 3.64 (t, J = 5.0 Hz, 4H), 1.73 (s, 4H), 1.50 (s, 4H); ^{13}C NMR (126 MHz, CDCl$_3$) δ 166.7, 156.2, 155.7, 153.0, 136.6, 134.9, 128.3, 125.7, 122.7, 120.5, 119.8, 111.7, 110.8, 102.3, 52.1, 27.9, 27.6; HRESI-MS m/z (M + H$^+$) Anal for C$_{20}$H$_{28}$N$_7$O$_3$: Calc. mass 393.2151. Found 393.2159; Anal HPLC (70:30 H$_2$O/0.1% TFA: CH$_3$CN/0.1% TFA→100% CH$_3$CN/0.1% TFA over 30 min, t_r =24.4 min).

3-Amino-5-(azepan-1-yl)-6-(benzo[b]thiophen-2-yl)-N-carbamimidoyl pyrazine-2-carboxamide (17)

General Method D using **17a** (383 mg, 1.0 mmol) gave **17** as a yellow solid; yield 78% (320 mg); MP 220-224 °C; ^{1}H NMR (500 MHz, CDCl$_3$) δ 10.48 (s, 1H), 8.92 (s, 2H), 8.76 (s, 2H), 7.60 (d, J = 7.5 Hz, 1H), 7.43 (d, J = 7.5 Hz, 1H), 7.31 (t, J = 7.5 Hz, 1H), 7.26 (t, J = 7.5 Hz, 1H), 7.20 (s, 1H), 3.50 (t, J = 5.75 Hz, 4H), 1.69 (s, 4H), 1.49 (s, 4H); ^{13}C NMR (126 MHz, CDCl$_3$) δ 168.2. 164.9, 160.7, 156.5, 155.4, 144.1, 141.3, 141.2, 125.8, 125.5, 124.7, 123.5, 123.0, 113.5, 52.0, 29.2, 28.1; HRESI-MS m/z (M + H$^+$) C$_{20}$H$_{24}$N$_7$OS: Calc. mass 410.1763. Found 410.1758; Anal. HPLC (100% H$_2$O/0.1% TFA→100% CH$_3$CN/0.1% TFA over 30 min, t_r 27.5 min).

3-Amino-5-(azepan-1-yl)-6-(benzofuran-2-yl)-N-carbamimidoylpyrazine-2-carboxamide (18)

General Method D using **18a** (366 mg, 1.0 mmol) gave **18** as a yellow solid; yield 86% (338 mg). MP 130-132 °C ; ^{1}H NMR (CD$_3$OD): δ 7.64 (d, J = 7.5 Hz, 1H), 7.50 (d, J = 8.0 Hz, 1H), 7.31 (t, J = 8.0 Hz, 1H), 7.26 (t, J = 7.5 Hz, 1H), 7.05 (s, 1H), 3.51 (t, J = 5.0 Hz, 4H), 1.71 (s, 4H), 1.54 (s, 4H); ^{13}C NMR (CD$_3$OD): δ 167.4, 164.3, 154.6, 154.5, 154.4, 154.1, 129.7, 124.9, 123.7, 121.6, 121.1, 112.4, 111.5, 105.6, 50.3, 28.6, 27.3; HRESI-MS m/z (M + H$^+$) Anal for C$_{20}$H$_{24}$N$_7$O$_2$: Calc. mass 394.1991. Found 394.1986; Anal HPLC (100% H$_2$O/0.1% TFA→100% CH$_3$CN/0.1% TFA over 30 min, t_r 27.5 min).

3-Amino-5-(azepan-1-yl)-N-carbamimidoyl-6-(4-fluorobenzofuran-2-yl)pyrazine-2-carboxamide (19)

General Method C using **19a** (54 mg, 0.139 mmol) gave **19** as an orange solid; yield 26% (15 mg, 0.036 mmol). MP: 132-136°C; ^{1}H NMR (500 MHz, CD$_3$OD) δ 10.47 (s, exchange with solvent), 8.98 (s, exchange with solvent), 8.33 (s, exchange with solvent), 7.36 (t, J = 8.7Hz, 1H), 7.32 (q, J = 5.5Hz, 1H), 7.22 (s, 1H), 7.02 (t, J = 8.7Hz, 1H), 3.44 (t, J = 5.8 Hz, 4H) 1.72 (s, 4H), 1.51 (s, 4H); ^{13}C NMR (126 MHz, CD$_3$OD) δ 167.3, 158.2, 157.4, 157.0, 156.9, 156.2, 156.2, 155.7, 126.6, 121.2, 112.2, 109.8, 108.7, 102.4, 51.1, 29.0, 27.9; HRESI-MS m/z (M + H$^+$) Anal for C$_{20}$H$_{22}$FN$_7$O$_2$,: Calc. mass 412.1897. Found 412.1909; Anal HPLC (70:30 H$_2$O/0.1% TFA: CH$_3$CN/0.1% TFA→100% CH$_3$CN/0.1% TFA over 30 min, t_r 25.6 min).

3-Amino-5-(azepan-1-yl)-N-carbamimidoyl-6-(thiophen-2-yl)pyrazine-2-carboxamide (20)

General Method C using **20a** (99 mg, 0.298 mmol) gave **20** as a yellow oil; yield 2% (2 mg, 0.006 mmol). MP 136-138 °C; ^{1}H NMR (500 MHz, CDCl$_3$) δ 10.10 (s, 1H), 10.04 (bs, 2H), 8.08 (bs, 2H), 7.26 (d, J = 5 Hz, 1H), 7.03 (d, J = 3 Hz, 1H), 3.47 (t, J = 5.75 Hz, 4H), 1.68 (m, 4H),

1.49 (m, 4H); ^{13}C NMR (126 MHz, CDCl$_3$) δ 167.0, 156.3, 156.1, 153.4, 139.9, 128.4, 128.2, 125.2, 124.5, 111.0, 51.0, 27.8, 27.1; HRESI-MS m/z (M + H$^+$) Anal for C$_{16}$H$_{21}$N$_7$O: Calc. mass 360.1607. Found 360.1610; Anal. HPLC (70:30 H$_2$O/0.1% TFA: CH$_3$CN/0.1% TFA→100% CH$_3$CN/0.1% TFA over 30 min, t_r 24.2 min).

3-Amino-5-(azepan-1-yl)-N-carbamimidoyl-6-(thiophen-3-yl)pyrazine-2-carboxamide (21)

General Method C using **21a** (103 mg, 0.309 mmol) gave **21** as an orange oil; yield 17% (24 mg, 0.067 mmol). MP: 138-140 °C; ^{1}H NMR (500 MHz, CDCl$_3$) δ 10.31 (s, 1H), 8.62 (bs, 2H), 8.29, (bs, 2H), 7.78 (m, 3H), 7.64 (dd, J = 8.5, 1.5 Hz, 1H,), 7.44 (m, 2H), 6.23 (bs, 2H), 3.38 (t, J = 5.75, 4H), 1.59 (s, 4H), 1.42 (s, 4H); ^{13}C NMR (126 MHz, CDCl$_3$) δ 166.7, 156.2, 156.0, 153.6, 140.1, 128.4, 127.8, 125.9, 123.6, 110.7, 51.3, 27.9, 27.1; HRESI-MS m/z (M + H$^+$) Anal for C$_{16}$H$_{21}$N$_7$O: Calc. mass 360.1607. Found 360.1611; Anal HPLC (70:30 H$_2$O/0.1% TFA: CH$_3$CN/0.1% TFA→100% CH$_3$CN/0.1% TFA over 30 min, t_r = 25.2 min).

3-Amino-5-(azepan-1-yl)-N-carbamimidoyl-6-(furan-2-yl)pyrazine-2-carboxamide (22)

General Method D using **22a** (316 mg, 1.0 mmol) gave **22** as a yellow solid; yield 91% (310 mg). MP 143-146 °C; ^{1}H NMR (CD$_3$OD): δ 7.50 (s, 1H), 6.55 (d, J = 3.0 Hz, 1H), 6.50 (s, 1H), 3.37 (t, J = 6.0 Hz, 4H), 1.64 (s, 4H), 1.47 (s, 4H); ^{13}C NMR (CD$_3$OD): δ 168.1, 160.7, 156.3, 156.0, 153.4, 142.8, 122.4, 112.6, 112.4, 109.9, 50.9, 29.2, 27.8. HRESI-MS m/z (M + H$^+$) Anal for C$_{16}$H$_{22}$N$_7$O$_2$: Calc. mass 344.1835. Found 344.1830; Anal HPLC (100% H$_2$O/0.1% TFA→100% CH$_3$CN/0.1% TFA over 30 min, t_r 24.3 min).

3-Amino-5-(azepan-1-yl)-N-carbamimidoyl-6-(furan-3-yl)pyrazine-2-carboxamide (23)

General Method C using **23a** (90 mg, 0.285 mmol) gave **23** as a yellow solid; yield 35% (41 mg, 0.119 mmol). MP 146-148 °C; ^{1}H NMR (500 MHz, CDCl$_3$) δ 10.42 (s, 1H), 8.54 (s, 4H), 7.63 (s, 1H), 7.42 (s, 1H), 6.63 (s, 1H), 5.35 (bs, 2H), 3.52 (t, J = 5.75 Hz, 4H), 1.68 (s, 4H), 1.49 (s, 4H); ^{13}C NMR (126 MHz, CDCl$_3$) δ 166.4, 156.3, 155.8, 153.6, 143.2, 141.1, 125.3, 124.9, 110.8, 110.7, 51.4, 27.9, 27.1; HRESI-MS m/z (M + H$^+$) Anal for C$_{16}$H$_{22}$N$_7$O$_2$: Calc. mass 344.1835. Found 344.1837; Anal HPLC (70:30 H$_2$O/0.1% TFA: CH$_3$CN/0.1% TFA→100% CH$_3$CN/0.1% TFA over 30 min, t_r 25.5 min).

3-Amino-5-(azepan-1-yl)-N-carbamimidoyl-6-(2-fluoropyridin-3-yl)pyrazine-2-carboxamide (24)

General Method C using **24a** (100 mg, 0.290 mmol) gave **24** as a yellow solid; yield 13% (18 mg, 0.048 mmol). MP 160-162 °C; ^{1}H NMR (500 MHz, CDCl$_3$) δ 10.42 (s, 1H), 8.59 (bs, 4H), 8.17 (m, 2H), 7.29 (t, J = 5.4 Hz) 5.13 (bs, 2H), 3.38 (s, 4H), 1.64 (s, 4H), 1.47 (s, 4H); ^{13}C NMR (126 MHz, CDCl$_3$) δ 166.5, 160.7, 158.8, 156.0, 155.9, 154.0, 146.9, 141.4, 124.2, 123.4, 122.5, 111.8, 50.4, 27.9, 27.2; HRESI-MS m/z (M + H$^+$) Anal for C$_{17}$H$_{22}$FN$_8$O: Calc. mass 373.1901. Found 373.1916; Anal HPLC (70:30 H$_2$O/0.1% TFA: CH$_3$CN/0.1% TFA→100% CH$_3$CN/0.1% TFA over 30 min, t_r 22.2 min).

3-Amino-5-(azepan-1-yl)-N-carbamimidoyl-6-(pyrimidin-5-yl)pyrazine-2-carboxamide (25)

General Method D using **25a** (328 mg, 1.0 mmol) gave **25** as a yellow solid; yield 87% (305 mg). MP 188-190 °C; ^{1}H NMR (CD$_3$OD): δ 8.98 (s, 1H), 8.97 (s, 2H), 3.35 (t, J = 5.5 Hz, 4H), 1.67 (s, 4H), 1.47 (s, 4H); ^{13}C NMR (CD$_3$OD): δ 162.2, 156.5, 156.3, 155.7, 155.5, 154.0, 153.5, 135.2, 122.2, 51.0, 28.0, 27.1; HRESI-MS m/z (M + H$^+$). Anal for C$_{16}$H$_{22}$N$_9$O: Calc. mass

356.1947.Found 356.1942; Anal HPLC (70:30 H$_2$O/0.1% TFA: CH$_3$CN/0.1% TFA→100% CH$_3$CN/0.1% TFA over 30 min, t_r 20.1 min).

3-Amino-5-(azepan-1-yl)-N-carbamimidoyl-6-(2-methoxypyrimidin-5-yl)pyrazine-2-carboxamide (26)

General Method D using **26a** (358 mg, 1.0 mmol) gave **26** as a yellow solid; yield 90% (345 mg). MP: 148-150 °C; ^{1}H NMR (CD$_3$OD): δ 8.77 (s, 2H), 4.08 (s, 3H), 3.46 (t, J = 5.5 Hz, 4H), 1.72 (s, 4H), 1.54 (s, 4H); ^{13}C NMR (CD$_3$OD): δ 166.7, 164.1, 163.4, 158.1, 154.8, 153.6, 128.6, 124.2, 112.8, 54.3, 27.7, 26.7; HRESI-MS m/z (M + H$^+$) Anal for C$_{17}$H$_{24}$N$_9$O$_2$: Calc. mass 386.2053. Found 386.2048; Anal HPLC (100% H$_2$O/0.1% TFA→100% CH$_3$CN/0.1% TFA over 30 min, t_r 20.7 min).

3-Amino-5-(azepan-1-yl)-N-carbamimidoyl-6-(2,4-dimethoxypyrimidin-5-yl)pyrazine-2-carboxamide (27)

General Method C using **27a** (104 mg, 0.267 mmol) gave **27** as a yellow solid; yield 54% (65 mg, 0.156 mmol). MP: 184-186 °C; ^{1}H NMR (CD$_3$OD) δ 10.76 (s, 1H), 9.27 (s, 2H), 8.51 (s, 2H), 8.48 (s, 2H), 4.08 (s, 3H), 3.35 (t, J = 5.75 Hz, 4H), 1.66 (s, 4H), 1.46 (s, 4H). ^{13}C NMR (126 MHz, CDCl$_3$) δ 166.6, 164.0, 157.8, 156.1, 153.9, 127.8, 124.7, 112.5, 55.6, 51.6, 27.8, 27.1; HRESI-MS m/z (M + H$^+$) Anal for C$_{18}$H$_{26}$N$_9$O$_3$: Calc. mass 416.2159. Found 416.2158; Anal HPLC (70:30 H$_2$O/0.1% TFA: CH$_3$CN/0.1% TFA→100% CH$_3$CN/0.1% TFA over 30 min, t_r 21.4 min).

3-Amino-5-(azepan-1-yl)-N-carbamimidoyl-6-(2,6-dimethoxypyridin-3-yl)pyrazine-2-carboxamide (28)

General Method C using **28a** (98 mg, 0.253 mmol) gave **28** as a yellow solid; yield 13% (15 mg, 0.036 mmol). MP: 152-154° C; ^{1}H NMR (500 MHz, CDCl$_3$) δ 10.28 (s, 1H), 8.77 (s, 2H), 8.14 (s, 2H), 7.61 (d, J = 8.0 Hz), 6.39 (d, J = 8.0 Hz, 1H), 3.94 (s, 3H), 3.87 (s, 3H), 3.52 (s, 2H), 3.35 (s, 2H), 1.60 (s, 4H), 1.51 (s, 2H), 1.44 (s, 2H); ^{13}C NMR (126 MHz, CDCl$_3$) δ 166.0, 163.2, 159.2, 155.4, 153.5, 141.1, 128.0, 114.6, 110.2, 101.3, 53.8, 53.5, 50.4, 27.7, 26.81; HRESI-MS *m/z* (M + H$^+$) Anal for C$_{19}$H$_{27}$N$_8$O$_3$: Calc. mass 415.2206. Found 415.2191; Anal HPLC (70:30 H$_2$O/0.1% TFA: CH$_3$CN/0.1% TFA→100% CH$_3$CN/0.1% TFA over 30 min, t_r 26.1 min).

3-Amino-5-(azepan-1-yl)-N-carbamimidoyl-6-(2,4-dimethoxyphenyl) pyrazine-2-carboxamide (29)

General Method C using **29a** (123 mg, 0.317 mmol) gave **29** as a yellow solid; yield 8% (12 mg, 0.029 mmol). MP: 156-158 °C; ^{1}H NMR (500 MHz, CDCl$_3$) δ 10.19 (s, 1H), 9.10 (bs, 2H), 7.79 (bs, 2H), 7.23 (d, *J* = 8.1 Hz), 6.58 (d, *J* = 8.1 Hz), 6.48 (s, 1H) 3.86 (s, 3H), 3.74 (s, 3H), 3.51 (s, 2H), 3.36 (s, 2H), 1.59 (s, 4H), 1.50 (s, 2H), 1.45 (s, 2H); ^{13}C NMR (126 MHz, CDCl$_3$) δ 166.0, 161.5, 157.8, 155.7, 155.4, 153.8, 130.6, 129.6, 122.1, 109.8, 105.0, 98.7, 55.7, 55.6, 50.6, 27.8, 26.9; HRESI-MS *m/z* (M + H$^+$) Anal for C$_{20}$H$_{28}$N$_7$O$_3$: Calc. mass 414.2254. Found 414.2269; Anal. HPLC (70:30 H$_2$O/0.1% TFA: CH$_3$CN/0.1% TFA→100% CH$_3$CN/0.1% TFA over 30 min, t_r 26.7 min).

3-Amino-5-(azepan-1-yl)-N-carbamimidoyl-6-(3,5-dimethoxyphenyl) pyrazine-2-carboxamide (30)

General Method C using **30a** (147 mg, 0.381 mmol) gave **30** as a yellow solid; yield 26% (44 mg, 0.116 mmol). MP: 138-140 °C; ^{1}H NMR (500 MHz, CDCl$_3$) δ 10.75 (s, 1H), 8.81 (bs, 2H), 8.60 (bs, 2H), 6.73 (d, J = 2.2 Hz), 6.58 (t, J = 2.2 Hz, 1H), 3.84 (s, 6H), 3.38 (s, 2H), 1.64 (s, 4H), 1.45 (s, 2H); ^{13}C NMR (126 MHz, CDCl$_3$) δ 167.0, 160.1, 156.4, 155.6, 153.8, 141.6, 132.9, 110.9, 106.5, 100.3, 55.9, 51.0, 28.0, 27.1; HRESI-MS m/z (M + H$^+$) Anal for C$_{20}$H$_{28}$N$_7$O$_3$: Calc. mass 414.2254. Found 414.2244; Anal. HPLC (70:30 H$_2$O/0.1% TFA: CH$_3$CN/0.1% TFA→100% CH$_3$CN/0.1% TFA over 30 min, t_r 25.8 min).

3-Amino-5-(azepan-1-yl)-N-carbamimidoyl-6-(3,6-dimethoxypyridazin-4-yl)pyrazine-2-carboxamide (31)

General Method C using 31a (94 mg, 0.243 mmol) gave **31** as a yellow solid; yield 17% (21 mg, 0.051 mmol). MP 202-204 °C; ^{1}H NMR (500 MHz, CD$_3$OD) δ 10.38 (s, exchange with solvent), 8.77 (s, exchange with solvent), 8.21 (s, exchange with solvent), 7.35 (s, 1H), 4.06 (s, 3H), 3.99 (s, 3H), 3.35 (s, 4H), 1.66 (s, 4H), 1.55 (s, 2H), 1.45 (s, 2H); ^{13}C NMR (126 MHz, CD$_3$OD) δ 167.3, 164.1, 160.9, 156.9, 156.8, 156.1, 136.3, 124.0, 121.4, 112.2, 55.4, 55.3, 51.0, 28.9, 27.9; HRESI-MS m/z (M + H$^+$) Anal for C$_{18}$H$_{26}$N$_9$O$_3$: Calc. mass 416.2159. Found 416.2150; Anal HPLC (70:30 H$_2$O/0.1% TFA: CH$_3$CN/0.1% TFA→00% CH$_3$CN/0.1% TFA over 30 min, t_r = 19.0 min).

3-Amino-6-(2-aminopyrimidin-5-yl)-5-(azepan-1-yl)-N-carbamimidoylpyrazine-2-carboxamide (32)

General Method D using **32a** (86 mg, 0.25 mmol) gave **32** as a yellow solid; yield 78% (72 mg). MP 225-228; ^{1}H NMR (DMSO-*d6*): δ 1.41 (s, 4H), 1.60 (s, 4H), 3.38 (t, *J* = 5.9 Hz, 4H), 6.73 (br s, 2H), 7.25 (br s, 1H), 8.40 (s, 2H); ^{13}C NMR (DMSO-*d6*): δ 167.5, 162.9, 159.1, 157.5, 154.9, 153.7, 126.0, 123.6, 112.9, 51.1, 28.0, 27.0; HRESI-MS *m/z* (M + H^{+}), Anal for $C_{16}H_{23}N_{10}O_3$: Calc. mass 371.2056. Found 371.2067; Anal. HPLC (100% H_2O/0.1% TFA→100% CH_3CN/0.1% TFA over 30 min, t_r 10.2 min).

3-Amino-5-(azepan-1-yl)-N-carbamimidoyl-6-(2-(methylamino)pyrimidin-5-yl)pyrazine-2-carboxamide (33)

General Method D using **33a** (39 mg, 0.11 mmol) gave **33** as a yellow solid; yield 85% (36 mg). MP 168-170; ^{1}H NMR (CD$_3$OD): δ 8.47 (s, 2H), 3.48 (t, *J* = 5.6 Hz, 4H), 2.97 (s, 3H), 1.69 (s, 4H), 1.51 (s, 4H); ^{13}C NMR (CD$_3$OD): δ 28.0, 28.5, 29.0, 52.0, 113.5, 124.4, 127.3, 155.4, 156.7, 158.3, 158.5, 162.9, 168.3, 162.9, 158.5, 158.3, 156.7, 155.4, 127.3, 124.4, 113.5, 52.0, 29.0, 28.5, 28.0; HRESI-MS *m/z* (M + H^{+}) Anal for $C_{17}H_{25}N_{10}O$: Calc. mass 385.2213, Found 385.2195; Anal. HPLC (100% H_2O/0.1% TFA→100% CH_3CN/0.1% TFA over 30 min, t_r 14.8 min).

3-Amino-5-(azepan-1-yl)-N-carbamimidoyl-6-(2-(isopropylamino)pyrimidin-5-yl)pyrazine-2-carboxamide (34)

General Method D using **34a** (35 mg, 0.09 mmol) gave **34** as a yellow solid; yield 89% (32 mg). MP: 172-175 °C; ^{1}H NMR (CD$_3$OD): δ 8.46 (s, 2H), 4.14 (septet, *J* = 6.8 Hz, 1H), 3.47 (t, *J* = 5.6 Hz, 4H), 1.69 (s, 4H), 1.51 (s, 4H), 1.25 (d, *J* = 6.5 Hz, 6H); ^{13}C NMR (CD$_3$OD): δ 21.6, 26.8, 27.8, 42.8, 50.9, 112.3, 123.2, 126.2, 154.2, 155.5, 157.1, 158.8, 160.6, 167.1, 160.6, 158.8,

157.1, 155.5, 154.2, 126.2, 123.3, 112.3, 50.9, 42.8, 27.8, 26.8, 21.6; HRESI-MS m/z (M + H$^+$)

Anal for $C_{19}H_{29}N_{10}O$: Calc. mass 413.2526, Found 413.2525; Anal. HPLC (100% H$_2$O/0.1%

TFA→100% CH$_3$CN/0.1% TFA over 30 min, t_r 16.1 min).

3-Amino-5-(azepan-1-yl)-N-carbamimidoyl-6-(2-((2-hydroxyethyl)amino)pyrimidin-5-yl)pyrazine-2-carboxamide (35)

General Method D using **35a** (50 mg, 0.13 mmol) gave **35** as a Yellow solid: yield 86% (46 mg).

MP: 188-191 °C; ^{1}H NMR (CD$_3$OD): δ 8.48 (s, 2H), 3.72 (t, J = 5.6 Hz, 2H),), 3.54 (t, J = 5.6

Hz, 2H), 3.45 (t, J = 5.8 Hz, 4H), 1.68 (s, 4H), 1.50 (s, 4H); ^{13}C NMR (CD$_3$OD): δ 167.1, 162.3,

160.8, 158.2, 156.3, 154.9, 126.5, 124.7, 117.5, 61.7, 51.9, 44.6, 28.9, 27.8.; HRESI-MS m/z (M

+ H$^+$) Anal for $C_{18}H_{27}N_{10}O_2$: Calc. mass 415.2318.Found 415.2324; Anal. HPLC (100%

H$_2$O/0.1% TFA→100% CH$_3$CN/0.1% TFA over 30 min, t_r 14.4 min).

Methyl 3-((di-tert-butyloxycarbonyl)amino)-5-(azepan-1-yl)-6-chloro-2-pyrazine carboxylate (36)

To a stirred solution of **7** (2.85 g, 10 mmol) and DMAP (61 mg, 0.5 mmol) in 1,2-dichloroethane (40 mL) was added a solution of di-*tert*-butyl dicarbonate (6.57 g, 30 mmol) in 1,2-dichloroethane (20 mL) at rt. The reaction mixture was heated at 70 °C for 18 h. After cooling to room temperature, additional equivalents of di-*tert*-butyl dicarbonate (3.28 g, 15 mmol) and DIPEA (10 mL) were added and the reaction mixture was heated for a further 18 h. Solvents were evaporated and the residue was partitioned between EtOAc (100 mL) and water (100 mL). The aqueous layer was extracted with EtOAc (3 x 75 mL) and the combined organic layer was washed with brine, dried (MgSO$_4$) and concentrated. The residue was purified by silica gel flash

column chromatography using EtOAc/pet spirit (10-15%) to give **36** (4.10 g, 85%) as a white solid; MP: 116-118 °C; ^{1}H NMR (CDCl$_3$): δ 3.89 (s, 3H), 3.88 (t, *J* = 6.1 Hz, 4H), 1.55 (s, 4H), 1.84 (s, 4H), 1.41 (s, 18H); ^{13}C NMR (CDCl$_3$): δ 163.0, 152.3, 150.4, 145.4, 128.6, 126.1, 83.3, 52.8, 51.6, 28.1, 28.1, 26.7; MS (ESI): m/z 507 (M+Na)$^+$; HRESI-MS *m/z* (M + H$^+$) Anal for C$_{22}$H$_{33}$ClN$_4$O$_6$Na: Calc. mass 507.1986. Found 507.2000; Anal. HPLC (100% H$_2$O/0.1% TFA→100% CH$_3$CN/0.1% TFA over 30 min).**Methyl 5-(azepan-1-yl)-3-((tert-butoxycarbonyl)amino)pyrazine-2-carboxylate (37)**

To a mixture of chloropyrazine **36** (3.30 g, 6.8 mmol), Pd/C (476 mg, 10 mol%) and MgO (408 mg, 10.2 mmol) was added dry MeOH (50 mL). The flask was charged with H$_2$ (1 atm) and the reaction mixture was stirred at rt for 2 days. The solvent was evaporated and the residue redissolved in EtOAc and filtered through Celite, eluting with EtOAc. The organic layer was washed with brine, dried (MgSO$_4$) and evaporated to give the crude mono Boc-protected product **37** as a white solid (2.22 g, 92%). Crude product showed sufficient purity and was used in the next step with further purification; MP: 97-100 °C; ^{1}H NMR (400 MHz, CDCl$_3$) δ 10.28 (s, 1H), 7.68 (s, 1H), 3.94 (s, 3H), 3.62 (br s, 4H), 1.58 (br s, 4H), 1.53 (s, 9H), 1.84 (br s, 4H); ^{13}C NMR (CDCl$_3$): δ 167.3, 153.8, 150.6, 150.3, 122.4, 113.5, 80.7, 52.3, 47.9, 28.3, 27.4, 26.6; HRESI-MS *m/z* (M + H$^+$) Anal for C$_{17}$H$_{27}$N$_4$O$_4$: 351.2032. Found 351.2032. Anal. HPLC (100% H$_2$O/0.1% TFA→100% CH$_3$CN/0.1% TFA over 30 min).

Methyl 5-(azepan-1-yl)-6-bromo-3-((tert-butoxycarbonyl)amino)pyrazine-2-carboxylate (38)

To a solution of pyrazine methyl ester **37** (2.10 g, 6.0 mmol) in CH$_2$Cl$_2$ (90 mL) was added *N*-bromosuccinimide (1.18 g, 6.6 mmol) and the reaction mixture was stirred at rt for 5 h. The

mixture was treated with water (50 mL) and stirred for 10 min. The organic layer was separated, washed with sodium bicarbonate solution (2 x 50 mL) and brine (50 mL), dried (MgSO$_4$) and concentrated. The residue was purified by silica gel flash column chromatography using EtOAc/pet spirit (10-15%) to give **38** (1.56 g, 60%) as a white solid; MP: 114-115 °C; ^{1}H NMR (CDCl$_3$): δ 10.04 (s, 1H), 3.95 (t, *J* = 6.0 Hz, 4H), 3.92 (s, 3H), 1.89 (br s, 4H), 1.60 (t, *J* = 3.1 Hz, 4H), 1.52 (s, 9H); ^{13}C NMR (CDCl$_3$): δ 166.3, 153.0, 150.0, 147.7, 114.8, 111.9, 81.0, 52.5, 51.4, 28.2, 28.2, 26.8; MS (ESI): m/z 429 (M+H)[+]; HRESI-MS *m/z* (M + Na^{+}) Anal for C$_{17}$H$_{25}$BrN$_4$O$_4$Na: Calc. mass 451.0957. Found 451.0959. Anal. HPLC (100% H$_2$O/0.1% TFA→100% CH$_3$CN/0.1% TFA over 30 min).

Methyl 5-(azepan-1-yl)-3-((tert-butoxycarbonyl)amino)-6-(pyrimidin-2-ylamino)pyrazine-2-carboxylate (39)

A re-sealable Schlenk tube was charged with bromopyrazine **38** (429 mg, 1.0 mmol), 2-aminopyrimidine (135 mg, 1.4 mmol), Pd$_2$(dba)$_3$ (10 mg, 0.011 mmol, 1 mol % Pd), Xantphos (13 mg, 0.022 mmol), Cs$_2$CO$_3$ (426 mg, 1.4 mmol) and degassed dioxane (5 mL). The Schlenk tube was capped and carefully subjected to three cycles of evacuation-backfilling with N$_2$. It was then sealed and the reaction mixture heated at 100 °C for 20 h. The mixture was cooled to rt, diluted with THF (20 mL), filtered through Celite and concentrated. The residue was purified by silica gel flash column chromatography using EtOAc/pet spirit (50-60%) to give **39** (130 mg, 30%) as a white solid; MP: 168-170 °C; ^{1}H NMR (CDCl$_3$): δ 10.16 (s, 1H), 8.35 (d, *J* = 4.8 Hz, 2H), 7.23 (s, 1H), 6.71 (t, *J* = 4.8 Hz, 1H), 3.90 (s, 3H), 3.77 (t, *J* = 6.0 Hz, 4H), 1.73 (br s, 4H), 1.53 (s, 9H), 1.48 (br s, 4H); ^{13}C NMR (CDCl$_3$): δ 166.8, 161.3, 158.3, 152.3, 150.2, 147.9, 126.6, 113.2, 111.5, 80.5, 52.4, 50.5, 28.3, 28.0, 26.8; MS (ESI): m/z 444 (M+H)[+]; HRESI-MS

m/z (M + H$^+$) Anal for C$_{21}$H$_{30}$N$_7$O$_4$: Calc. mass 444.2359. Found 444.2374. Anal. HPLC (100% H$_2$O/0.1% TFA→100% CH$_3$CN/0.1% TFA over 30 min).

Methyl 3-amino-5-(azepan-1-yl)-6-(pyrimidin-2-ylamino)pyrazine-2-carboxylate (40)

To a solution of Boc-protected pyrazine **39** (60 mg, 0.135 mmol) in CH$_2$Cl$_2$ (4 mL) at 0 °C was added TFA (0.1 mL) and the mixture was stirred at room temperature overnight. The mixture was concentrated *in vacuo* and the residue partitioned between CH$_2$Cl$_2$ (20 mL) and saturated NaHCO$_3$ solution (20 mL). The organic layer was dried (MgSO$_4$) and concentrated and the residue purified by silica gel flash column chromatography using EtOAc/pet spirit (60-70%) to give **40** (45 mg, 98%) as a grey solid; MP: 194-196 °C; ^{1}H NMR (CDCl$_3$): δ 8.34 (d, *J* = 4.8 Hz, 2H), 7.04 (s, 1H), 6.67 (t, *J* = 4.8 Hz, 1H), 6.20 (br s, 2H, NH$_2$), 3.87 (s, 3H), 3.67 (t, *J* = 6.0 Hz, 4H), 1.69 (br s, 4H), 1.48 (t, *J* = 3.2 Hz, 4H); ^{13}C NMR (CDCl$_3$): δ 166.8, 161.8, 158.4, 154.2, 153.5, 124.3, 112.8, 109.4, 52.0, 50.6, 50.3, 28.2, 26.7; HRESI-MS *m/z* (M + H$^+$) Anal for C$_{16}$H$_{22}$N$_7$O$_2$: Calc. mass 344.1835. Found 344.1848. Anal. HPLC (100% H$_2$O/0.1% TFA→100% CH$_3$CN/0.1% TFA over 30 min).

3-Amino-5-(azepan-1-yl)-N-carbamimidoyl-6-(pyrimidin-2-ylamino)pyrazine-2-carboxamide (41)

General Method D using **40** (35 mg, 0.1 mmol) gave **41** (30 mg, 81%) as a yellow solid: MP: 210-212 °C; ^{1}H NMR (CD$_3$OD): δ 8.25 (d, *J* = 4.9 Hz, 2H), 6.70 (t, *J* = 4.9 Hz, 1H), 3.70 (t, *J* = 6.0 Hz, 4H), 1.63 (br s, 4H), 1.43 (t, *J* = 3.1 Hz, 4H); ^{13}C NMR (CD$_3$OD): δ 165.7, 162.2, 158.3, 155.6, 154.9, 154.8, 124.1, 112.3, 108.0, 50.4, 27.8, 26.2; MS (ESI): m/z 371 (M+H)$^+$; HRESI-

MS m/z (M + H$^+$) Anal for $C_{16}H_{23}N_{10}O$: Calc. mass 371.2056. Found 371.2057; Anal HPLC (100% H$_2$O/0.1% TFA→100% CH$_3$CN/0.1% TFA over 30 min, t_r = 14.3 min).

Cell culture conditions. ATCC certified cell lines were used for all experiments. Cells were cultured at 37 °C, 95% humidity and 5% (v/v) CO$_2$ in a ThermoScientific Heracell 150i CO$_2$ incubator (ThermoScientific) and maintained in DMEM/Hi Glucose culture medium supplemented with 10% heat-inactivated FCS. Adherent cells were passaged via the addition of trypsin/0.05% EDTA solution (GIBCO), followed by centrifugation and resuspension in fresh media using a 5 mL Luerlock syringe fitted with an 18-gauge needle (Terumo, Tokyo, Japan). All cell lines were obtained from ATCC certified stocks and routinely tested for the presence of mycoplasma infection.

Fluorometric uPA activity assay. Urokinase from human kidney cells (Cat # U4010, Sigma-Aldrich, St. Louis, MI, USA) was diluted to 900 nM, aliquoted and stored at -80 °C until use in experiments (typically 4-5 plates assayed on the same day). Thawed enzyme stocks were maintained at -20 °C between during assays using a Nalgene Labtop Cooler Jr (Cat# 5115-0012, Thermo-Fisher Scientific, Waltham, Massachusetts, USA). A 5 mM stock solution of Urokinase fluorescent substrate III (Z-Gly-Gly-Arg-AMC, Calbiochem Cat # 672159, Merck Millipore, Massachusetts, USA, Human uPA K_m = 400 µM) was prepared in dH$_2$O/10% DMSO and aliquoted with storage at -20 °C. Assay buffer (20 mM HEPES pH 7.4, 100 mM NaCl, 0.5 mM EDTA, 0.01% v/v Tween-20) was prepared and used within 7 days with storage at 4 °C. On the day of assay, compound stocks (20-50 mM in anhydrous DMSO) were serially diluted in assay buffer in a clear Greiner CELLSTAR$^®$ 96-well plate on ice (Greiner Bio-One GmBH,

Kremsmünster, Austria) to give each dilution at 2X the final assayed concentration. In a separate black Greiner CELLSTAR® 96-well plate (Greiner Bio-One GmBH, Kremsmünster, Austria), residual volumes of assay buffer were added via multichannel pipette to compound fluorescence blanks and inhibited enzyme control wells, as appropriate. Next, 90 µL of dilute fluor (250 µM final) was added to all wells, followed by 100 µL of 2x compound dilution to appropriate wells. Immediately prior to assay, 900 nM uPA stock was diluted to 15 nM and 10 µL of this dilution was added to all relevant wells, initiating the reaction. Reaction progress was monitored using a POLARStar OMEGA fluorescence plate reader (Fluorescence intensity mode, top-optic, ex. 355 nm em. 450 nm, 20 flashes per well, double orbital shaking for 3s prior to every read, cycle time 60 s, 45-60 cycles, incubation at 37 °C, BMG-Labtech, Ortenberg, Germany). Changes in fluorescence over a 15 minute period from the linear portion of the reaction progress curve were used to determine IC_{50} values by fitting log-transformed data to a sigmoidal dose-response curve in GraphPad PRISM v7.0 (GraphPad Software, La Jolla, CA, USA). Experiments with Mouse uPA (Active Mouse Urokinase, HMW, Molecular Innovations Inc., Michigan, USA) were performed as above with a final enzyme concentration of 20 nM ($K_m = 580$). K_i values were calculated according to the methods of Cheng and Prussof.[54]

Chromogenic Trypsin-like serine protease (TLSP) activity assays. For experiments using uPA (Cat # U4010, Sigma-Aldrich, St. Louis, MI, USA), trypsin, tPA, thrombin, plasmin and Factor Xa, concentrated stocks were prepared in deionized H_2O and stored at -80 °C until thawed for use. Thawed enzyme stocks were maintained at -20 °C between assays using a Nalgene Labtop Cooler Jr (Cat# 5115-0012, Thermo-Fisher Scientific, Waltham, Massachusetts, USA). A 312.5 µM stock solution of S-2288 chromogenic substrate (H-D-Ile-L-Pro-L-Arg-*p*-nitoraniline, Chromogenix, Massachusettes, USA, uPA $K_m = 200$ µM, trypsin $K_m = 28$ µM, tPA $K_m = 300$

μM, thrombin K_m = 3 μM, plasmin K_m = 9 mM) was prepared in deionized H_2O and aliquoted with storage at -20 °C. Assay buffer (10 mM HEPES, 150 mM NaCl, 0.01% v/v Tween-20, pH 7.4) was prepared and used within 7 days with storage at 4 °C. On the day of assay, compound stocks (20-50 mM in DMSO) were serially diluted in assay buffer in a clear Greiner CELLSTAR® 96-well plate on ice (Greiner Bio-One GmBH, Kremsmünster, Austria) to give each dilution at 10X the final assay concentration. In a separate Greiner CELLSTAR® 96-well plate (Greiner Bio-One GmBH, Kremsmünster, Austria) residual volumes of assay buffer were added via multi-channel pipette to compound fluorescence blanks and inhibited enzyme control wells, as appropriate. Next, 80 μL of dilute substrate (250 μM final) was added to all wells, followed by 10 μL of 10x compound dilution to appropriate wells. Immediately prior to assay, concentrated enzyme stocks were diluted to 100 nM and 10 μL of this dilution was added to all relevant wells, initiating the reaction (Final enzyme concentration = 10 nM). DMSO was present at a final concentration of 1% v/v. Change in absorbance over time at 405 nm was measured at 37 °C using a Molecular Devices SpectraMax Plus 384-well plate reader (Molecular Devices LLC, Sunnyvale, California, USA). IC_{50} values were determined by plotting percentage of residual activity (V0) versus log drug concentration and fitted to sigmoidal dose response curves using GraphPad PRISM v7.0 (GraphPad Software, La Jolla, CA, USA). The following chromogenic substrates and final enzyme concentrations were used for experiments with other TLSPs. S-2366, L-pyroGlu-L-Pro-L-Arg-*p*-nitroaniline, Chromogenix, Massachusettes, USA, [Human plasma kallikrein] = 23.5 nM, K_m = 430 μM, [Factor XIa] = 2 nM, K_m = 400 μM, [Activated protein C] = 10 nM, K_m = 200 μM.

Crystallization and X-ray Data Collection. Expression and purification of recombinant human uPA protease domain was performed as previously described[79]. Crystals were grown by

the sitting drop vapor diffusion method and were obtained by equilibrating against a reservoir solution containing 50 mM sodium citrate (pH 4.6) and 2.0 M ammonium sulfate supplemented with 5% PEG400 at room temperature for a period of 3 days. For uPA:inhibitor co-complexes at pH 7.4, the crystals were soaked for one week in new soaking buffer (40% PEG4000, 100 mM Tris-HCl pH 7.4) containing 100 μM compound. Prior to X-ray data collection, crystals were soaked in a cryoprotectant solution containing 20% glycerol and snap-frozen in liquid N_2. X-ray diffraction data of the crystals were collected at the BL17U beamline, Shanghai Synchrotron Radiation Facility (SSRF). The diffraction data was indexed and integrated using the HKL2000 program package[80]. Structures were solved by molecular replacement[81] using the uPA structure (PDB code: 4DVA)[82] as the search model. The electron density for the compound was clearly visible in the uPA active sites and was modelled based on the F_o-F_c difference map. The structures was refined using the ccp4 program package[80] and manually adjusted using the molecular graphics program COOT[83] iteratively until convergence. Solvent molecules were added using a F_o-F_c Fourier difference map at 2.5 σ in the final refinement step. Statistics for data collection and final model refinement are summarized in the Supporting Information Table S1.

EnPlex assays. Enplex superfamily-wide serine hydrolase activity screening was performed as described in reference 56.

Cytotoxicity assays. Sub-confluent cells (~70-80% confluence) were harvested and dissociated into a single cell suspension. Cells were seeded at a density of 5000 cells/well (final volume 90 μl) into a Greiner CELLSTAR® 96-well plate (Greiner Bio-One GmBH,

Kremsmünster, Austria) via multichannel pipette and incubated for 18h prior to the addition of compounds. Compounds were serially diluted from 20-50 mM DMSO stocks in culture media in a separate 96-well plate under sterile conditions to give 10x stocks (10 nM-1 mM) on the day of compound addition. 10 µL of the 10x compound/media stocks or matched vehicle/media solutions (for vehicle controls; final vehicle concentration was equal to 0.2%) were transferred via multichannel pipette into the assay plate containing 90 µL cell suspension via multichannel pipette to give the treated assay plate at the final 1X drug concentrations (1 nM-100 µM, $n = 4$ wells at each concentration). Drug blanks or vehicle media blanks were included as appropriate at each concentration to correct for intrinsic color of the compounds and the Phenol Red containing media. 200 µL media was added to outside wells to decrease evaporation but were not used in the assay itself. Compound-treated plates were incubated for 48h prior to development. After 48h, plates were removed from the incubator and 20 µL CellTitre 96® Aqueous One Solution Cell Proliferation Assay (Cat # G3581, Promega Corporation, Fitchburg, Wisconsin, USA) was added to each well. Plates were incubated for a further 2h prior to reading at 490 nm using a SpectraMax Plus 384-well plate reader (Molecular Devices LLC, Sunnyvale, California, USA). IC_{50} values (defined as the concentration of each treatment causing 50% inhibition of maximal cell viability) were determined using a logarithmic sigmoidal dose-response curve using the variable slope parameter to determine IC_{50} using GraphPad PRISM v7.0 (GraphPad Software, La Jolla, CA, USA).

ENaC inhibition assays. HEK-293 Cells were cultured in Dulbecco's Modified Eagle Medium/Nutrient Mixture F-12 (D-MEM/F-12) supplemented with 10% fetal bovine serum, 100 U/mL penicillin G sodium, 100 µg/mL streptomycin sulfate and appropriate selection antibiotics.

Semi-confluent cells were transfected with cDNA for ENaC α, β and γ subunits (genes SCNN1A, SCNN1B and SCNN1G) prior to experimentation. Cells were plated at a density of 20,000 cells/well in a 384-well black wall, flat clear bottom microtiter plates (Type: BD Biocoat Poly-D-Lysine Multiwell Cell Culture Plate) and incubated at 37 ℃ overnight. Following manufacturer instructions, cells were loaded with 20 µL of membrane potential dye solution for 30 min at 37 °C from the FLIPR Membrane Potential Red Dye Fluorescence Assay Kit (Molecular Devices, Sunnyvale, California, USA). This assay uses fluorometric detection of changes in membrane potential following modulation of transmembrane ion channel/exchanger activity; i.e. antagonism of stimulated ENaC activity in this case. Drug, vehicle and control solutions were prepared from frozen stocks in DMSO on the day of experimentation through dilution into HEPES-buffered physiological salt solution (NaCl 137 mM, KCl 4 mM, $CaCl_2$ 1.8 mM, $MgCl_2$ 1 mM, HEPES 10 mM, Glucose 10 mM, DMSO 0.3% v/v, pH 7.4) in a 384-well microtiter plate ready for addition to the assay plate by the FLIPR^{TETRA} instrument. All analogs were tested at 8 concentrations (n = 4 wells at each concentration). Positive control cells were stimulated with 1 µM S-3969 (ENaC agonist, n = 4 wells)[84]. Negative control cells were first stimulated with 1 µM S-3969 and then treated with 30 µM benzamil (potent ENaC antagonist, n = 4 wells). Following dye loading, cells were pre-incubated with 5 µL drug, vehicle or control solutions for 5 min. Next 5 µL of S-3939 solution (final [S-3969] = 1 µM) was added to stimulate ENaC activity. All data were normalized to agonist-treated positive and antagonist-treated negative controls such that the agonist-treated signal corresponded to 100% activity and antagonist-treated signal corresponded to 0% activity. Normalized data were used to determine IC_{50} values for each analog using the log[inhibitor]-normalized response variable slope algorithm in GraphPad PRISM v7.0 (GraphPad Software, La Jolla, California, USA). These experiments

were performed under contract by Charles River Laboratories, Cleveland, Ohio, USA.

Rat diuresis and kaliuresis model. Sixty-four male 21 week old Sprague-Dawley rats were randomised into 8 groups of 8 animals. All test animals received one intraperitoneal (IP) injection of either vehicle or 25 mg/kg Acetazolamide followed by one intravenous (IV) injection of vehicle, 1.5 mg/kg Amiloride or 1.5 mg/kg Amiloride derivative. Acetazolamide was administered at an injection volume of 1 ml/kg and concentration of 25 mg/ml. Amiloride, HMA, **18** and **26** were administered at an injection volume of 1 ml/kg and concentration of 1.5 mg/ml. Monosodium acetazolamide was formulated in 0.9% saline. Amiloride and HMA were formulated in 50 mM acetate buffer (pH 5.5)/5% v/v DMSO, **18** and **26** were formulated in 50 mM acetate buffer (pH 5.5)/5% v/v DMSO/0.5% v/v Tween-80. Immediately following dosing, all animals were placed into metabolic cages and total urine collected over 6 h. A control group receiving IP and IV administrations of vehicle was also included for comparison. Urine Na^+ and K^+ levels were quantitated using a Konelab 20 XTi Biochemistry Analyzer (LLQ = 20 mM). This experiment was approved by the Austin Health Animal Ethics Committee (A2016/05420) and was conducted in accordance with the Australian Code of Practice for the Care and Use of Animals for Scientific Purposes, 7th Edition, 2004. Statistical analyses were performed using a one-way ANOVA with Dunnett's post-hoc test in GraphPad PRISM v7.0 (GraphPad Software, La Jolla, California, USA).

Mouse lung metastasis model. All animal studies were approved by the Institutional Animal Care and Use Committee at the University of Wollongong (AE1708). Male and female NOD.Cg-Prkdc<scid>IL2rg<tm1Wjl>SzJAusb mice (Australian BioResources, Moss Vale, NSW,

Australia) at 7-8 weeks of age were randomized into treatment groups (n = 4-6/treatment group). Treatments commenced one day prior to tail vein administration of 2.5×10^5 luciferase-tagged HT-1080 human fibrosarcoma cells (BioWare Brite HT-1080-Red-Fluc) in an injection volume of 100 uL PBS [Except sham control ($n = 1$)]. Daily IP injections continued to day 20 with 7.5 mg/kg amiloride, **18**, **26** or vehicle (50 mM acetate buffer pH 5.5, 7.5% v/v DMSO, 0.75% Tween-80). Animals were weighed and assessed for clinical signs daily. Humane endpoints of >15% acute weight loss (from previous 7 day maximum individual weight) or >20% chronic weight loss (from all-time individual maximum weight) or a body condition score >3 were employed. On day 21, all remaining animals were euthanized via slow CO_2 asphyxiation, weighed, necropsied and had their lungs removed. Lungs were snap frozen in liquid N_2 and stored at -80 °C until homogenization. Lungs were homogenized on ice using a PRO Scientific Bio-Gen PRO200 Homogenizer in cell lysis buffer (150 mM NaCl, 10 mM Tris Base, 1% Triton X100 v/v, pH 8.0) and centrifuged twice at 4 °C and 1,000 rpm for 15 min to remove cell debris. Homogenates were prepared to approximately 50 mg/mL protein based on individual wet lung weights. Luciferase activity was quantified according to the manufacturer's instructions using the Molecular Diagnostics SpectraMax Glo Steady-Luc Report Assay Kit. Luciferase assays were conducted in clear-bottomed white walled 96 well plates (Nunc) using a BMG Labtech PolarSTAR multimode plate reader. Data were analysed using GraphPad PRISM v7.0 and statistical significance determined using the one-way ANOVA with Dunnett's Post-hoc test.

Orthotopic model of pancreatic cancer. The orthotopic model has been described in detail previously.[69, 85] In brief, 6–8-week-old female athymic nude mice (BALB/c nu/nu) were anaesthetised and an incision was made in the left flank, followed by exteriorisation of the spleen

and tail of the pancreas. A mixture of human PC cells (AsPC-1) 1×10^6 + human PSCs (hPSCs) 1×10^6 in $50\,\mu$l PBS was injected into the tail of the pancreas. AsPC-1 cells were chosen for their high implantation rate (100% in our hands) and high reproducibility of tumor growth rates and metastasis. After intra-pancreatic injection, organs were reinternalized and the abdomen surgically closed. Mice receiving treatment were randomised into subgroups (n = 4 mice per group) on postsurgical day 7. These mice were treated as follows for 4 weeks: Gemcitabine (75 mg/Kg BIW oral gavage); **18** or **26** (10 mg/kg/day IP or Vehicle (daily IP, BIW oral gavage). Compounds were formulated for IP injection in 50 mM sodium acetate buffer (pH 5.5)/10% (v/v) DMSO/1% (w/v/) Kolliphor HS-15 and filtered through 0.22 μm PVDF syringe-driven filters under sterile conditions. Pancreatic tumor growth was monitored by palpation. Mice were killed at 4 weeks after first IP injection. Tumors were resected and assessed for size and volume by two separate observers (tumor volume was calculated to two decimal points, according to an established formula (1/2(length × breadth × width) using digital Vernier calipers (Intech tools, Thomas town, VIC, Australia)[85]. The abdominal cavity, mesentery, spleen, liver and lungs were examined and scored according to the presence or absence of visible macrometastatic nodules. these organs were then excised and fixed in 10% neutral buffered formalin overnight and processed using the Leica Peloris Dual Retort tissue processor (Germany). Histological staining was performed on 4μm sections deparaffinised in xylene and rehydrated using graded ethanol washes. Haematoxylin and Eosin staining were performed on a Leica Autostainer XL.

This experiment was approved by the University of New South Wales Animal Care and Ethics Committee (Approval number 15/106A) and was conducted in accordance with ARRIVE Guidelines.

ASSOCIATED CONTENT

Supporting Information

The Supporting Information is available free of charge on the ACS Publications website at DOI: XXXXX

> X-ray crystallography refinement data and statistics, HT-1080 uPA and uPAR expression data, experimental late-stage metastasis model clinical score sheet and histology images. Molecular formula strings of all compounds (CSV).

AUTHOR INFORMATION

Corresponding Authors

*M.K.: e-mail, mkelso@uow.edu.au; phone, +61 2 4221 5085.

*M.R.: e-mail, mranson@uow.edu.au; phone, +61 2 4221 3291.

ORCID

Michael J. Kelso: 0000-0001-7809-6637

Marie Ranson: 0000-0002-5570-9645

ABBREVIATIONS USED

ABPP, Activity-based protein profiling; ASIC1a, Acid-sensing ion channel 1a; *C1r*, complement C1r subcomponent; *C1s*, Complement component 1s; *DDHD1*, Phosphatidic acid-preferring phospholipase A1; DIPEA, Diisopropylethylamine; DOCA, Deoxycorticosterone acetate; *DPP7*, Dipeptidyl peptidase 2; ENaC, Epithelial sodium channel; *FLT3*-ITD+, Fms-like tyrosine kinase internal tandem duplication positive; GABA-A, γ-aminobutyric acid$_A$ receptor; Gem , Gemcitabine; GIRK, G protein-coupled inwardly-rectifying potassium channel; GnRHR, Gonadotropin-releasing hormone receptor; GPCR, G protein-coupled receptor; hA$_{2A}$AR-WT, Human adenosine A$_{2A}$ receptor; HER2, Human epidermal growth factor receptor 2; HIV-1, Human immunodeficiency virus 1; HMA, 5- (*N*,*N*-hexamethylene) amiloride; Hpsc, Human pancreatic stellate cells; *KLKb1*, Plasma kallikrein; *LACTB*, Serine beta-lactamase-like protein; NECA, 5'-(*N*-ethylcarboxamido)adenosine; NHE1, Sodium hydrogen exchanger isoform 1; NSB Non-specific binding; P2X$_7$, P2X purinoreceptor; *PRCP*, prolylcarboxypeptidase; SOSA, Selective optimization of side-activity; SAR, Structure-activity relationship; SAPE, Streptavidin-phycoerythrin; TB, total binding; TLSP, Trypsin-like serine protease; *TMPRSS11d*, Trypsin and transmembrane protease serine 11D; uPA, Urokinase plasminogen activator; uPAR, Urokinase plasminogen activator receptor.

REFERENCES

1.   Ulisse, S.; Baldini, E.; Sorrenti, S.; D'Armiento, M., The urokinase plasminogen activator system: a target for anti-cancer therapy. *Curr. Cancer. Drug. Targets.* **2009**, *9* (1), 32-71.
2.   Brungs, D.; Chen, J.; Aghmesheh, M.; Vine, K. L.; Becker, T. M.; Carolan, M. G.; Ranson, M., The urokinase plasminogen activation system in gastroesophageal cancer: A systematic review and meta-analysis. *Oncotarget* **2017**, *8* (14), 23099-23109.
3.   Croucher, D. R.; Saunders, D. N.; Lobov, S.; Ranson, M., Revisiting the biological roles of PAI2 (SERPINB2) in cancer. *Nat. Rev. Cancer.* **2008**, *8* (7), 535-545.
4.   Harris, N. L. E.; Vennin, C.; Conway, J. R. W.; Vine, K. L.; Pinese, M.; Cowley, M. J.; Shearer, R. F.; Lucas, M. C.; Herrmann, D.; Allam, A. H.; Pajic, M.; Morton, J. P.; Australian Pancreatic Cancer Genome, I.; Biankin, A. V.; Ranson, M.; Timpson, P.; Saunders, D. N., SerpinB2 regulates stromal remodelling and local invasion in pancreatic cancer. *Oncogene* **2017**, *36* (30), 4288-4298.
5.   Yang, J. L.; Seetoo, D.; Wang, Y.; Ranson, M.; Berney, C. R.; Ham, J. M.; Russell, P. J.; Crowe, P. J., Urokinase-type plasminogen activator and its receptor in colorectal cancer: independent prognostic factors of metastasis and cancer-specific survival and potential therapeutic targets. *Int J Cancer* **2000**, *89* (5), 431-439.
6.   Harris, L.; Fritsche, H.; Mennel, R.; Norton, L.; Ravdin, P.; Taube, S.; Somerfield, M. R.; Hayes, D. F.; Bast, R. C., Jr., American society of clinical oncology 2007 update of recommendations for the use of tumor markers in breast cancer. *J. Clin. Oncol.* **2007**, *25* (33), 5287-5312.
7.   Look, M. P.; van Putten, W. L.; Duffy, M. J.; Harbeck, N.; Christensen, I. J.; Thomssen, C.; Kates, R.; Spyratos, F.; Ferno, M.; Eppenberger-Castori, S.; Sweep, C. G.; Ulm, K.; Peyrat, J. P.; Martin, P. M.; Magdelenat, H.; Brunner, N.; Duggan, C.; Lisboa, B. W.; Bendahl, P. O.; Quillien, V.; Daver, A.; Ricolleau, G.; Meijer-van Gelder, M. E.; Manders, P.; Fiets, W. E.; Blankenstein, M. A.; Broet, P.; Romain, S.; Daxenbichler, G.; Windbichler, G.; Cufer, T.; Borstnar, S.; Kueng, W.; Beex, L. V.; Klijn, J. G.; O'Higgins, N.; Eppenberger, U.; Janicke, F.; Schmitt, M.; Foekens, J. A., Pooled analysis of prognostic impact of urokinase-type plasminogen activator and its inhibitor PAI-1 in 8377 breast cancer patients. *J. Natl. Cancer. Inst.* **2002**, *94* (2), 116-128.
8.   Foekens, J. A.; Peters, H. A.; Look, M. P.; Portengen, H.; Schmitt, M.; Kramer, M. D.; Brunner, N.; Janicke, F.; Meijer-van Gelder, M. E.; Henzen-Logmans, S. C.; van Putten, W. L.; Klijn, J. G., The urokinase system of plasminogen activation and prognosis in 2780 breast cancer patients. *Cancer. Res.* **2000**, *60* (3), 636-643.
9.   Duffy, M. J.; O'Grady, P.; Devaney, D.; O'Siorain, L.; Fennelly, J. J.; Lijnen, H. J., Urokinase-plasminogen activator, a marker for aggressive breast carcinomas. Preliminary report. *Cancer* **1988**, *62* (3), 531-533.
10.   Estreicher, A.; Muhlhauser, J.; Carpentier, J. L.; Orci, L.; Vassalli, J. D., The receptor for urokinase type plasminogen activator polarizes expression of the protease to the leading edge of migrating monocytes and promotes degradation of enzyme inhibitor complexes. *J. Cell. Biol.* **1990**, *111* (2), 783-792.
11.   Lund, I. K.; Illemann, M.; Thurison, T.; Christensen, I. J.; Hoyer-Hansen, G., uPAR as anti-cancer target: evaluation of biomarker potential, histological localization, and antibody-based therapy. *Curr. Drug. Targets.* **2011**, *12* (12), 1744-1760.

12.   Dohn, L. H.; Illemann, M.; Høyer-Hansen, G.; Christensen, I. J.; Hostmark, J.; Litlekalsoy, J.; von der Maase, H.; Pappot, H.; Laerum, O. D., Urokinase-type plasminogen activator receptor (uPAR) expression is associated with T-stage and survival in urothelial carcinoma of the bladder. *Urol. Oncol.* **2015**, *33* (4), 165.e15-24.

13.   Ploug, M.; Ellis, V., Structure-function relationships in the receptor for urokinase-type plasminogen activator. Comparison to other members of the Ly-6 family and snake venom alpha-neurotoxins. *FEBS Lett.* **1994**, *349* (2), 163-168.

14.   Duffy, M. J.; Duggan, C., The urokinase plasminogen activator system: a rich source of tumour markers for the individualised management of patients with cancer. *Clin. Biochem.* **2004**, *37* (7), 541-548.

15.   Rowe, R. G.; Weiss, S. J., Navigating ECM barriers at the invasive front: the cancer cell-stroma interface. *Annu. Rev. Cell. Dev. Biol.* **2009**, *25*, 567-595.

16.   Matthews, H.; Ranson, M.; Kelso, M. J., Anti-tumour/metastasis effects of the potassium-sparing diuretic amiloride: an orally active anti-cancer drug waiting for its call-of-duty? *Int. J. Cancer.* **2011**, *129* (9), 2051-2061.

17.   Ranson, M.; Andronicos, N. M., Plasminogen binding and cancer: promises and pitfalls. *Front. Biosci.* **2003**, *8*, s294-304.

18.   Ngo, J. C.; Jiang, L.; Lin, Z.; Yuan, C.; Chen, Z.; Zhang, X.; Yu, H.; Wang, J.; Lin, L.; Huang, M., Structural basis for therapeutic intervention of uPA/uPAR system. *Curr. Drug. Targets.* **2011**, *12* (12), 1729-1743.

19.   Tyndall, J. D.; Kelso, M. J.; Clingan, P.; Ranson, M., Peptides and small molecules targeting the plasminogen activation system: towards prophylactic anti-metastasis drugs for breast cancer. *Recent. Pat. Anticancer. Drug. Discov.* **2008**, *3* (1), 1-13.

20.   Towle, M. J.; Lee, A.; Maduakor, E. C.; Schwartz, C. E.; Bridges, A. J.; Littlefield, B. A., Inhibition of urokinase by 4-substituted benzo[b]thiophene-2-carboxamidines: an important new class of selective synthetic urokinase inhibitor. *Cancer. Res.* **1993**, *53* (11), 2553-2559.

21.   Xing, R. H.; Mazar, A.; Henkin, J.; Rabbani, S. A., Prevention of breast cancer growth, invasion, and metastasis by antiestrogen tamoxifen alone or in combination with urokinase inhibitor B-428. *Cancer. Res.* **1997**, *57* (16), 3585-3593.

22.   Alonso, D. F.; Tejera, A. M.; Farias, E. F.; Bal de Kier Joffe, E.; Gomez, D. E., Inhibition of mammary tumor cell adhesion, migration, and invasion by the selective synthetic urokinase inhibitor B428. *Anticancer. Res.* **1998**, *18* (6a), 4499-4504.

23.   Nienaber, V. L.; Davidson, D.; Edalji, R.; Giranda, V. L.; Klinghofer, V.; Henkin, J.; Magdalinos, P.; Mantei, R.; Merrick, S.; Severin, J. M.; Smith, R. A.; Stewart, K.; Walter, K.; Wang, J.; Wendt, M.; Weitzberg, M.; Zhao, X.; Rockway, T., Structure-directed discovery of potent non-peptidic inhibitors of human urokinase that access a novel binding subsite. *Structure* **2000**, *8* (5), 553-563.

24.   Wendt, M. D.; Geyer, A.; McClellan, W. J.; Rockway, T. W.; Weitzberg, M.; Zhao, X.; Mantei, R.; Stewart, K.; Nienaber, V.; Klinghofer, V.; Giranda, V. L., Interaction with the S1 beta-pocket of urokinase: 8-heterocycle substituted and 6,8-disubstituted 2-naphthamidine urokinase inhibitors. *Bioorg. Med. Chem. Lett.* **2004**, *14* (12), 3063-3068.

25.   Wendt, M. D.; Rockway, T. W.; Geyer, A.; McClellan, W.; Weitzberg, M.; Zhao, X.; Mantei, R.; Nienaber, V. L.; Stewart, K.; Klinghofer, V.; Giranda, V. L., Identification of novel binding interactions in the development of potent, selective 2-naphthamidine inhibitors of urokinase. Synthesis, structural analysis, and SAR of N-phenyl amide 6-substitution. *J. Med. Chem.* **2004**, *47* (2), 303-324.

26.   Bruncko, M.; McClellan, W. J.; Wendt, M. D.; Sauer, D. R.; Geyer, A.; Dalton, C. R.; Kaminski, M. A.; Weitzberg, M.; Gong, J.; Dellaria, J. F.; Mantei, R.; Zhao, X.; Nienaber, V. L.; Stewart, K.; Klinghofer, V.; Bouska, J.; Rockway, T. W.; Giranda, V. L., Naphthamidine urokinase plasminogen activator inhibitors with improved pharmacokinetic properties. *Bioorg Med. Chem. Lett.* **2005**, *15* (1), 93-98.
27.   Rockway, T. W.; Giranda, V. L., Inhibitors of the proteolytic activity of urokinase type plasminogen activator. *Curr. Pharm. Des.* **2003**, *9* (19), 1483-1498.
28.   Frederickson, M.; Callaghan, O.; Chessari, G.; Congreve, M.; Cowan, S. R.; Matthews, J. E.; McMenamin, R.; Smith, D. M.; Vinkovic, M.; Wallis, N. G., Fragment-based discovery of mexiletine derivatives as orally bioavailable inhibitors of urokinase-type plasminogen activator. *J. Med. Chem.* **2008**, *51* (2), 183-186.
29.   Sturzebecher, J.; Vieweg, H.; Steinmetzer, T.; Schweinitz, A.; Stubbs, M. T.; Renatus, M.; Wikstrom, P., 3-Amidinophenylalanine-based inhibitors of urokinase. *Bioorg. Med. Chem. Lett.* **1999**, *9* (21), 3147-3152.
30.   Heinemann, V.; Ebert, M. P.; Laubender, R. P.; Bevan, P.; Mala, C.; Boeck, S., Phase II randomised proof-of-concept study of the urokinase inhibitor upamostat (WX-671) in combination with gemcitabine compared with gemcitabine alone in patients with non-resectable, locally advanced pancreatic cancer. *Br. J. Cancer.* **2013**, *108* (4), 766-770.
31.   AG, W., Positive Phase II data for MESUPRON® in breast cancer. *Wilex Half-Yearly Financial Report 2012* **2012**.
32.   Spinar, J.; Spinarova, L.; Vitovec, J., Diuretics in monotherapy and in combination with other diuretics and nondiuretics in the treatment of hypertension. *Vnitr. Lek.* **2013**, *59* (6), 486-494.
33.   Lant, A. F.; Smith, A. J.; Wilson, G. M., Clinical evaluation of amiloride, a potassium-sparing diuretic. *Clin. Pharmacol. Ther.* **1969**, *10* (1), 50-63.
34.   Kleyman, T. R.; Cragoe, E. J., Jr., The mechanism of action of amiloride. *Semin. Nephrol.* **1988**, *8* (3), 242-248.
35.   Palmer, B. F., Regulation of Potassium Homeostasis. *Clin. J. Am. Soc. Nephrol.* **2015**, *10* (6), 1050-1060.
36.   Jankun, J.; Keck, R. W.; Skrzypczak-Jankun, E.; Swiercz, R., Inhibitors of urokinase reduce size of prostate cancer xenografts in severe combined immunodeficient mice. *Cancer. Res.* **1997**, *57* (4), 559-563.
37.   Vassalli, J. D.; Belin, D., Amiloride selectively inhibits the urokinase-type plasminogen activator. *FEBS Lett.* **1987**, *214* (1), 187-191.
38.   Perazella, M. A., Drug-induced hyperkalemia: old culprits and new offenders. *Am. J. Med.* **2000**, *109* (4), 307-314.
39.   Wermuth, C. G., Selective optimization of side activities: another way for drug discovery. *J. Med. Chem.* **2004**, *47* (6), 1303-1314.
40.   Matthews, H.; Ranson, M.; Tyndall, J. D.; Kelso, M. J., Synthesis and preliminary evaluation of amiloride analogs as inhibitors of the urokinase-type plasminogen activator (uPA). *Bioorg. Med.Chem. Lett.* **2011**, *21* (22), 6760-6766.
41.   Kleyman, T. R.; Cragoe, E. J., Jr., Amiloride and its analogs as tools in the study of ion transport. *J. Membr. Biol.* **1988**, *105* (1), 1-21.
42.   Song, C. W.; Lyons, J. C.; Makepeace, C. M.; Griffin, R. J.; Cragoe, E. J., Jr., Effects of HMA, an analog of amiloride, on the thermosensitivity of tumors in vivo. *Int. J. Radiat. Oncol. Biol. Phys.* **1994**, *30* (1), 133-139.

43.   Luo, J.; Tannock, I. F., Inhibition of the regulation of intracellular pH: potential of 5-(N,N-hexamethylene) amiloride in tumour-selective therapy. *Br. J. Cancer.* **1994**, *70* (4), 617-624.

44.   Rich, I. N.; Worthington-White, D.; Garden, O. A.; Musk, P., Apoptosis of leukemic cells accompanies reduction in intracellular pH after targeted inhibition of the Na(+)/H(+) exchanger. *Blood* **2000**, *95* (4), 1427-1434.

45.   Man, C. H.; Lam, S. S.; Sun, M. K.; Chow, H. C.; Gill, H.; Kwong, Y. L.; Leung, A. Y., A novel tescalcin-sodium/hydrogen exchange axis underlying sorafenib resistance in FLT3-ITD+ AML. *Blood* **2014**, *123* (16), 2530-2539.

46.   Ye, J. H.; Gao, J.; Wu, Y. N.; Hu, Y. J.; Zhang, C. P.; Xu, T. L., Identification of acid-sensing ion channels in adenoid cystic carcinomas. *Biochem. Biophys. Res. Commun.* **2007**, *355* (4), 986-992.

47.   Rowson-Hodel, A. R.; Berg, A. L.; Wald, J. H.; Hatakeyama, J.; VanderVorst, K.; Curiel, D. A.; Leon, L. J.; Sweeney, C.; Carraway, K. L., Hexamethylene amiloride engages a novel reactive oxygen species- and lysosome-dependent programmed necrotic mechanism to selectively target breast cancer cells. *Can. Lett.* **2016**, *375* (1), 62-72.

48.   Kleyman, T. R.; Cragoe, E. J., Jr., Cation transport probes: the amiloride series. *Methods Enzymol.* **1990**, *191*, 739-755.

49.   Cragoe, E. J.; Woltersdorf, O. W.; Bicking, J. B.; Kwong, S. F.; Jones, J. H., Pyrazine Diuretics. II. N-Amidino-3-amino-5-substituted 6-Halopyrazinecarboxamides. *J. Med. Chem.* **1967**, *10* (1), 66-75.

50.   Patwardhan, N. N.; Ganser, L. R.; Kapral, G. J.; Eubanks, C. S.; Lee, J.; Sathyamoorthy, B.; Al-Hashimi, H. M.; Hargrove, A. E., Amiloride as a new RNA-binding scaffold with activity against HIV-1 TAR. *Med. Chem. Comm.* **2017**, *8* (5), 1022-1036.

51.   Zeslawska, E.; Schweinitz, A.; Karcher, A.; Sondermann, P.; Sperl, S.; Sturzebecher, J.; Jacob, U., Crystals of the urokinase type plasminogen activator variant beta(c)-uPAin complex with small molecule inhibitors open the way towards structure-based drug design. *J. Mol. Biol.* **2000**, *301* (2), 465-475.

52.   Lee, S.; Yi, K. Y.; Hwang, S. K.; Lee, B. H.; Yoo, S.-e.; Lee, K., (5-Arylfuran-2-ylcarbonyl)guanidines as cardioprotectives through the inhibition of Na+/H+ exchanger isoform-1. *J. Med. Chem.* **2005**, *48* (8), 2882-2891.

53.   Cochran, B. J.; Gunawardhana, L. P.; Vine, K. L.; Lee, J. A.; Lobov, S.; Ranson, M., The CD-loop of PAI-2 (SERPINB2) is redundant in the targeting, inhibition and clearance of cell surface uPA activity. *BMC Biotechnol.* **2009**, *9*, 43, 1-9.

54.   Yung-Chi, C.; Prusoff, W. H., Relationship between the inhibition constant (KI) and the concentration of inhibitor which causes 50 per cent inhibition (I50) of an enzymatic reaction. *Biochem. Pharmacol.* **1973**, *22* (23), 3099-3108.

55.   Nienaber, V.; Wang, J.; Davidson, D.; Henkin, J., Re-engineering of human urokinase provides a system for structure-based drug design at high resolution and reveals a novel structural subsite. *J. Biol. Chem.* **2000**, *275* (10), 7239-7248.

56.   Bachovchin, D. A.; Koblan, L. W.; Wu, W.; Liu, Y.; Li, Y.; Zhao, P.; Woznica, I.; Shu, Y.; Lai, J. H.; Poplawski, S. E.; Kiritsy, C. P.; Healey, S. E.; DiMare, M.; Sanford, D. G.; Munford, R. S.; Bachovchin, W. W.; Golub, T. R., A high-throughput, multiplexed assay for superfamily-wide profiling of enzyme activity. *Nat. Chem. Biol.* **2014**, *10* (8), 656-663.

57.   Soisson, S. M.; Patel, S. B.; Abeywickrema, P. D.; Byrne, N. J.; Diehl, R. E.; Hall, D. L.; Ford, R. E.; Reid, J. C.; Rickert, K. W.; Shipman, J. M.; Sharma, S.; Lumb, K. J., Structural

definition and substrate specificity of the S28 protease family: the crystal structure of human prolylcarboxypeptidase. *BMC. Struct. Biol.* **2010**, *10*, 16, 1-8.

58. Soudijn, W.; Van Wijngaarden, I.; AP, I. J., Allosteric modulation of G protein-coupled receptors: perspectives and recent developments. *Drug. Discov. Today.* **2004**, *9* (17), 752-758.

59. Gao, Z. G.; Ijzerman, A. P., Allosteric modulation of A(2A) adenosine receptors by amiloride analogues and sodium ions. *Biochem. Pharmacol.* **2000**, *60* (5), 669-676.

60. Garritsen, A.; Beukers, M. W.; Ijzerman, A. P.; Soudijn, W., Recognition of adenosine receptors by amiloride and its analogues. *Nucleosides Nucleotides* **1991**, *10* (5), 1107-1111.

61. Garritsen, A.; Ijzerman, A. P.; Tulp, M. T.; Cragoe, E. J., Jr.; Soudijn, W., Receptor binding profiles of amiloride analogues provide no evidence for a link between receptors and the Na+/H+ exchanger, but indicate a common structure on receptor proteins. *J. Recept. Res.* **1991**, *11* (6), 891-907.

62. de Lera Ruiz, M.; Lim, Y.-H.; Zheng, J., Adenosine A2A receptor as a drug discovery target. *J. Med. Chem.* **2014**, *57* (9), 3623-3650.

63. Massink, A.; Louvel, J.; Adlere, I.; van Veen, C.; Huisman, B. J.; Dijksteel, G. S.; Guo, D.; Lenselink, E. B.; Buckley, B. J.; Matthews, H.; Ranson, M.; Kelso, M.; AP, I. J., 5'-Substituted amiloride derivatives as allosteric modulators binding in the sodium ion pocket of the adenosine A2A receptor. *J. Med. Chem.* **2016**, *59* (10), 4769-4777.

64. Klinghofer, V.; Stewart, K.; McGonigal, T.; Smith, R.; Sarthy, A.; Nienaber, V.; Butler, C.; Dorwin, S.; Richardson, P.; Weitzberg, M.; Wendt, M.; Rockway, T.; Zhao, X.; Hulkower, K. I.; Giranda, V. L., Species specificity of amidine-based urokinase inhibitors. *Biochemistry* **2001**, *40* (31), 9125-9131.

65. McNay, J. L.; Oran, E., Possible predisposition of diabetic patients to hyperkalemia following administration of potassium-retaining diuretic, amiloride (MK 870). *Metabolism* **1970**, *19* (1), 58-70.

66. Baer, J. E.; Jones, C. B.; Spitzer, S. A.; Russo, H. F., The potassium-sparing and natriuretic activity of N-amidino-3,5-diamino-6-chloropyrazinecarboxamide hydrochloride dihydrate (amiloride hydrochloride). *J. Pharmacol. Exp. Ther.* **1967**, *157* (2), 472-485.

67. Comprehensive pharmacokinetic profiling of compounds **18** and **26** will be reported elsewhere.

68. Uhland, K.; Siphos, B.; Arkona, C.; Schuster, M.; Petri, B.; Steinmetzer, P.; Mueller, F.; Schweinitz, A.; Steinmetzer, T.; Van De Locht, A., Use of IHC and newly designed matriptase inhibitors to elucidate the role of matriptase in pancreatic ductal adenocarcinoma. *Int. J. Oncol.* **2009**, *35* (2), 347-357.

69. Pothula, S. P.; Xu, Z.; Goldstein, D.; Biankin, A. V.; Pirola, R. C.; Wilson, J. S.; Apte, M. V., Hepatocyte growth factor inhibition: a novel therapeutic approach in pancreatic cancer. *Br. J. Cancer.* **2016**, *114* (3), 269-280.

70. Nikishkin, N. I.; Huskens, J.; Verboom, W., Transition metal-catalyzed functionalization of pyrazines. *Org. Biomol. Chem.* **2013**, *11* (22), 3583-3602.

71. Chessell, I. P.; Michel, A. D.; Humphrey, P. P., Properties of the pore-forming P2X7 purinoceptor in mouse NTW8 microglial cells. *Br. J. Pharmacol.* **1997**, *121* (7), 1429-1437.

72. Amith, S. R.; Wilkinson, J. M.; Fliegel, L., KR-33028, a potent inhibitor of the Na(+)/H(+) exchanger NHE1, suppresses metastatic potential of triple-negative breast cancer cells. *Biochem. Pharmacol.* **2016**, *118*, 31-39.

73. Rosenberg, M. R.; Weaver, L. M.; Casarotto, M. G., Probing interactions of Vpu from HIV-1 with amiloride-based compounds. *Biochim. Biophys. Acta.* **2016**, *1858* (4), 733-739.

74.   Jalily, P. H.; Eldstrom, J.; Miller, S. C.; Kwan, D. C.; Tai, S. S.-H.; Chou, D.; Niikura, M.; Tietjen, I.; Fedida, D., Mechanisms of action of novel influenza A/M2 viroporin inhibitors derived from hexamethylene amiloride. *Mol. Pharmacol.* **2016**, *90* (2), 80-95.

75.   Heitman, L. H.; Ye, K.; Oosterom, J.; Ijzerman, A. P., Amiloride derivatives and a nonpeptidic antagonist bind at two distinct allosteric sites in the human gonadotropin-releasing hormone receptor. *Mol. Pharmacol.* **2008**, *73* (6), 1808-1815.

76.   Snell, H. D.; Gonzales, E. B., 5-(N, N-Hexamethylene) amiloride is a GABA-A ρ1 receptor positive allosteric modulator. *Channels* **2016**, *10* (6), 498-506.

77.   Leng, T. D.; Si, H. F.; Li, J.; Yang, T.; Zhu, M.; Wang, B.; Simon, R. P.; Xiong, Z. G., Amiloride analogs as ASIC1a inhibitors. *CNS. Neurosci. Ther.* **2016**, *22* (6), 468-476.

78.   Cox, G.; Ewart, G.; Gage, P., A Method of Modulating Ion Channel Functional Activity. PCT Int. Appl. WO2000021538 A1, Ed. 2000.

79.   Zhao, G.; Yuan, C.; Wind, T.; Huang, Z.; Andreasen, P. A.; Huang, M., Structural basis of specificity of a peptidyl urokinase inhibitor, upain-1. *J. Struct. Biol.* **2007**, *160* (1), 1-10.

80.   Otwinowski, Z.; Minor, W., Processing of X-ray diffraction data collected in oscillation mode. *Methods. Enzymol.* **1997**, *276*, 307-326.

81.   CCP4, The CCP4 suite; Programs for protein crystallography. *Acta. Cryst.* **1994**, *D50*, 760-763.

82.   Jiang, L.; Botkjaer, K. A.; Andersen, L. M.; Yuan, C.; Andreasen, P. A.; Huang, M., Rezymogenation of active urokinase induced by an inhibitory antibody. *Biochem. J.* **2013**, *449* (1), 161-166.

83.   Emsley, P.; Cowtan, K., Coot: model-building tools for molecular graphics. *Acta. Crystallogr. D Biol. Crystallogr.* **2004**, *60* (Pt 12 Pt 1), 2126-2132.

84.   Lu, M.; Echeverri, F.; Kalabat, D.; Laita, B.; Dahan, D. S.; Smith, R. D.; Xu, H.; Staszewski, L.; Yamamoto, J.; Ling, J.; Hwang, N.; Kimmich, R.; Li, P.; Patron, E.; Keung, W.; Patron, A.; Moyer, B. D., Small molecule activator of the human epithelial sodium channel. *J. Biol. Chem.* **2008**, *283* (18), 11981-11994.

85.   Xu, Z.; Vonlaufen, A.; Phillips, P. A.; Fiala-Beer, E.; Zhang, X.; Yang, L.; Biankin, A. V.; Goldstein, D.; Pirola, R. C.; Wilson, J. S.; Apte, M. V., Role of pancreatic stellate cells in pancreatic cancer metastasis. *Am. J. Pathol.* **2010**, *177* (5), 2585-2596.